ASE-1372

A PROGRAM OF X-RAY ASTRONOMY

FROM SOUNDING ROCKETS

H. Gursky
R. Giacconi
P. Gorenstein
J. R. Waters

Prepared under Contract No. NASW-1284 by

American Science and Engineering, Inc.
11 Carleton Street, Cambridge, Massachusetts 02142

for

NATIONAL AERONAUTICS AND SPACE ADMINISTRATION

FOREWORD

This document is the final report on NASA contract NASW-1284. This contract is part of a continuing program of X-ray astronomy by AS&E and called for the design, fabrication and flight of two instrumented payloads from Aerobee rockets and preliminary analysis of the resulting data.

ACKNOWLEDGMENTS

We wish to acknowledge the contributions of the following individuals at AS&E to this program. Mr. A. DeCaprio, the project Mechanical Engineer; Mr. H. Manko, the project Systems Engineer; and Mr. S. Mickiewicz, the project Electronic Engineer, were responsible for the design, fabrication and testing of the payloads in their respective areas. Additional engineering support was obtained from Mr. W. Antrim, Director of the Mechanical Department, Mr. B. Johnson, Director of the Electronics Department, and Mr. G. Sinnamon, Director of the Systems Department. Mr. G. Ouellette carried out many of the astronomical calculations needed in the program and Mr. M. Bate was responsible for the computer programming and much of the analytical work associated with the data analysis.

We also wish to acknowledge many fruitful discussions with Dr. Martin Annis, Dr. Jack Carpenter, and Dr. Oscar Manley of AS&E and Professor Bruno Rossi of MIT.

Portions of this work represented a joint effort with scientists at MIT. In particular, Professors M. Oda, H. Bradt, G. Garmire and Dr. R. V. Sreekantan made important contributions to the program.

TABLE OF CONTENTS

LIST OF FIGURES

LIST OF TABLES

1.0 INTRODUCTION

39 991

The work performed during this program resulted in the flight of scientific payloads on two Aerobee rockets, numbers 4.147 and 4.148. As a result of data obtained during these flights, it has been possible to locate the visible counterpart of ScoX-1, the bright X-ray source in Scorpio. This result may be sufficient to solve the problem of the nature of some of the galactic X-ray sources. The visible object is bright (12^{th} mag) and has many of the properties associated with old novae. AUTHOR

2.0 EXPERIMENT PLAN 4.147

The flight of Aerobee 4.147 was scheduled for late in 1965 and was to carry a suitably refurbished payload originally developed under contract NASW-898 and flown on Aerobees 4.122 & 4.123.

The limited capability of this payload in terms of available detector area and control made the choice of a suitable experiment difficult. The following rocket experiments had been flown during 1965.

a. NRL. Low resolution survey using despun rocket. Rocket motion consisted of low spin rate and large precession cone.

b. Lockheed. High resolution survey using an attitude controlled (ACS) rocket. Rocket was allowed to scan along the galactic equator and through the region containing ScoX-1, the strong source in Scorpio.

c. ASE. High resolution survey using spinning rocket. Rocket motion consisted of high spin rate and small precession cone.

These experiments had established the following facts regarding the X-ray sources.

a. NRL. Observation of a number of sources with a high concentration in region ($\pm 20^{o}$) around the galactic center, two sources in Cygnus and one source in Serpens. Source locations were given, but precision was low (several degrees).

b. Lockheed Essentially the same results as the NRL experiment. High resolution was obtained along the galactic equator yielding locations that confined the sources to a narrow (1^{o}) band normal to the galactic equator. Combining NRL and Lockheed data allowed refinement of the locations of a number of the X-ray sources.

c. AS&E - MIT. Similar results to those obtained above, except that principal scan was normal to the galactic equator. Two sources along galactic were located within about a 1 square degree box and it was established that all the sources in the vicinity of the galactic center were within several degrees of the galactic equator. The angular size of ScoX-1 was measured to be less than 7 arc minutes.

The locations of these sources is summarized in Figure 1. The outstanding feature of the distribution of the sources is the confinement to the galactic equator and the clustering in the vicinity of the galactic center. In both the AS&E and NRL experiments a large expanse of the remainder of the celestial sphere was scanned with no indication of X-ray sources of near comparable intensity. Aside from the theoretical implications of this observation, from an experimental point of view, it meant that the most significant data would be obtained by confining the observation to the galactic equator.

Such a scan is actually possible from White Sands Missile Range with an Aerobee rocket without the necessity of an ACS. This results from the fact, observed in our own previous flights, that the rocket (provided it is not deliberately despun) retained its original (prelaunch) heading within several degrees throughout the flight and until reentry into the atmosphere, i.e.: a rocket launched from WSMR, which is at a latitude of $+33^{\circ}$ (actual experience indicated that it would lay over North by several degrees) and would end up above the atmosphere at a declination close to $+33^{\circ}$. The galactic pole is at $+27^{\circ}$. declination, thus if the rocket were fired at a sidereal time corresponding to the Right Ascension of the pole ($12^{n}\ 50^{m}$) the rocket heading would be within 10° of the galactic pole and a detector mounted 90° to the heading axis would scan along a great circle that was tilted by at most 10° to

X-RAY SOURCE LOCATIONS

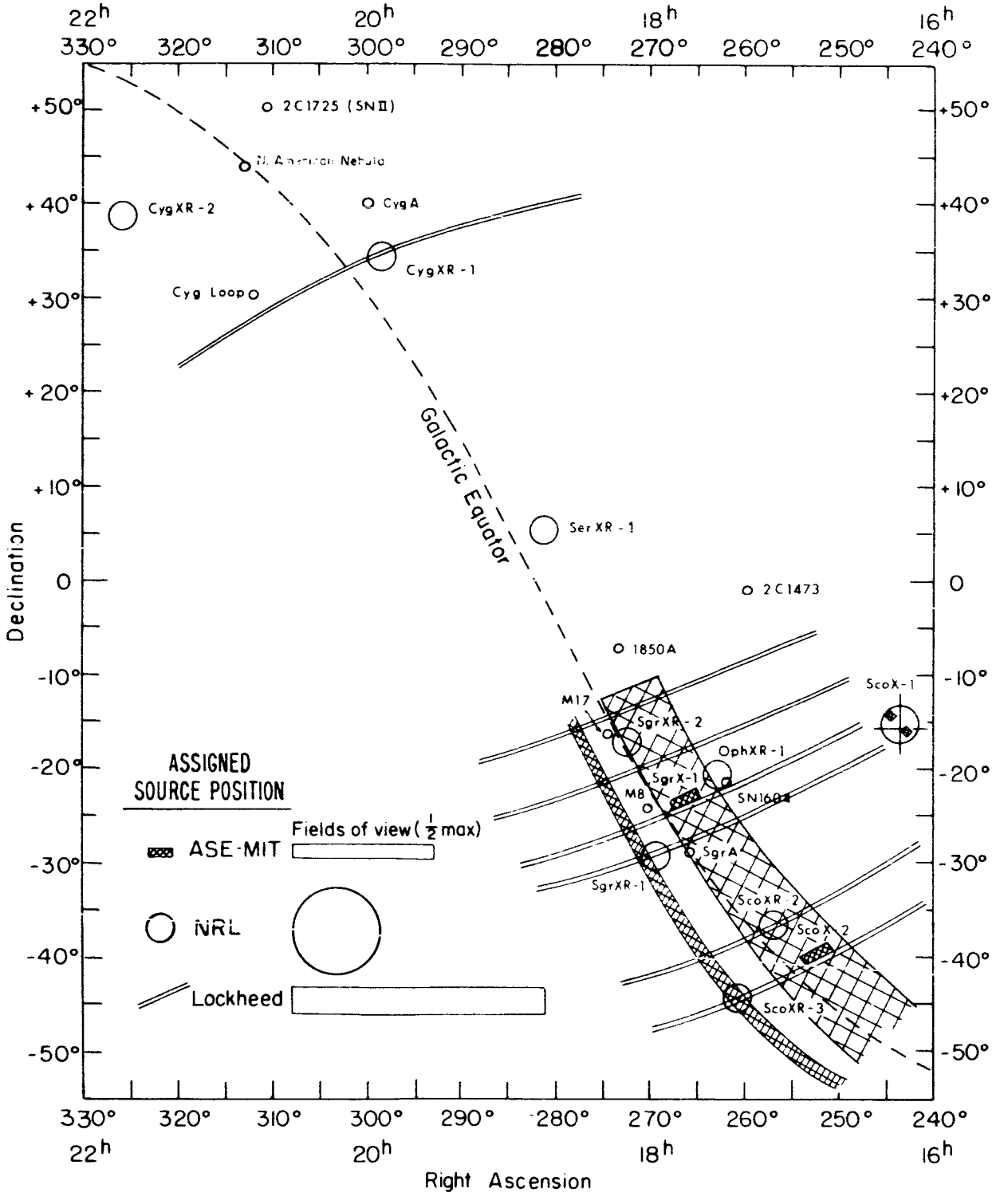

Figure 1

the galactic equator. In actual fact, since only a certain portion of the galactic equator is of interest (from Scorpio to Cygnus) a flight time can be chosen that minimizes the angular deviation between the two great circles. There is a potential serious problem with absorption in the residual atmosphere. The scan circle corresponds approximately to the horizon, 90° from the zenith. At this angle the mass of residual atmosphere, integrated along the line of sight, is about 30 times what it is in the zenith direction. The actual mass is a very strong function of both zenith angle and altitude.

We developed a means of calculating the atmospheric absorption as a function of both altitude and detector elevation which is outlined in Appendix I. The data contained in Appendix I were considered when making the choice of the launch time in order to assure that no source was unobservable because of absorption. From these considerations it was clear that a scan along the galactic equator could be achieved from a spinning rocket, provided the detector field of view was large enough in the direction normal to the galactic equator to allow for the actual scan circle being as much as 10° off the galactic equator.

There still remained the question of an actual experiment. The relevant parameters that one can measure are:

1. Location
2. Angular Size
3. Spectral Content

The actual payload restricts the precision with which these quantities can be measured. In order to achieve an adequate signal from the sources the opening angle of collimators was made at least 2°. This meant that during a 300 second rocket flight approximately 1.5 seconds was spent on each resolution interval.

One set of counters was collimated to look along a line normal to the scan direction; another set of counters was collimated to look along a line 60° off the scan direction.

Angular size can be measured with the use of modulation collimators as was done in the AS&E experiment conducted under contract NASW-898. Within the confines of this particular payload we used a modulation collimator whose angular resolution was 8 arc minutes. Depending on the signal/noise ratio when looking at a given source, an upper limit of as little as 1 to 2 arc minutes can be placed on angular size.

Spectral information can be obtained with the use of proportional counters. In previous experiments we had used a combination of geiger counters plus filters to obtain spectral data in the range 1-10 kev, and scintillation counters to obtain data in the range 10 kev. In this experiment we used proportional counters with a Xenon gas filling. Because of the use of Xenon, the efficiency for X-ray absorption extends significantly beyond 10 kev as is shown in Figure 2, and allows the entire spectral range to be covered with a single detector.

The spectral resolution is poor, particularly at low energy; however, the primary intent of the experiment is to observe qualitative differences in the spectral content of the various sources. In order to improve the quality of the data at low energy (1.5 kev) a thin aluminum filter was incorporated in front of one set of counters that was transported in front of the second set of counters midway during the flight. This filter, because of the X-ray absorption edge at 1.5 kev, absorbs a major portion of the incident X-rays at energies between 1.5 and about 4 kev, whereas its effect at other energies are negligible. Comparison of counting rates with and without the filter allows an unambiguous statement regarding

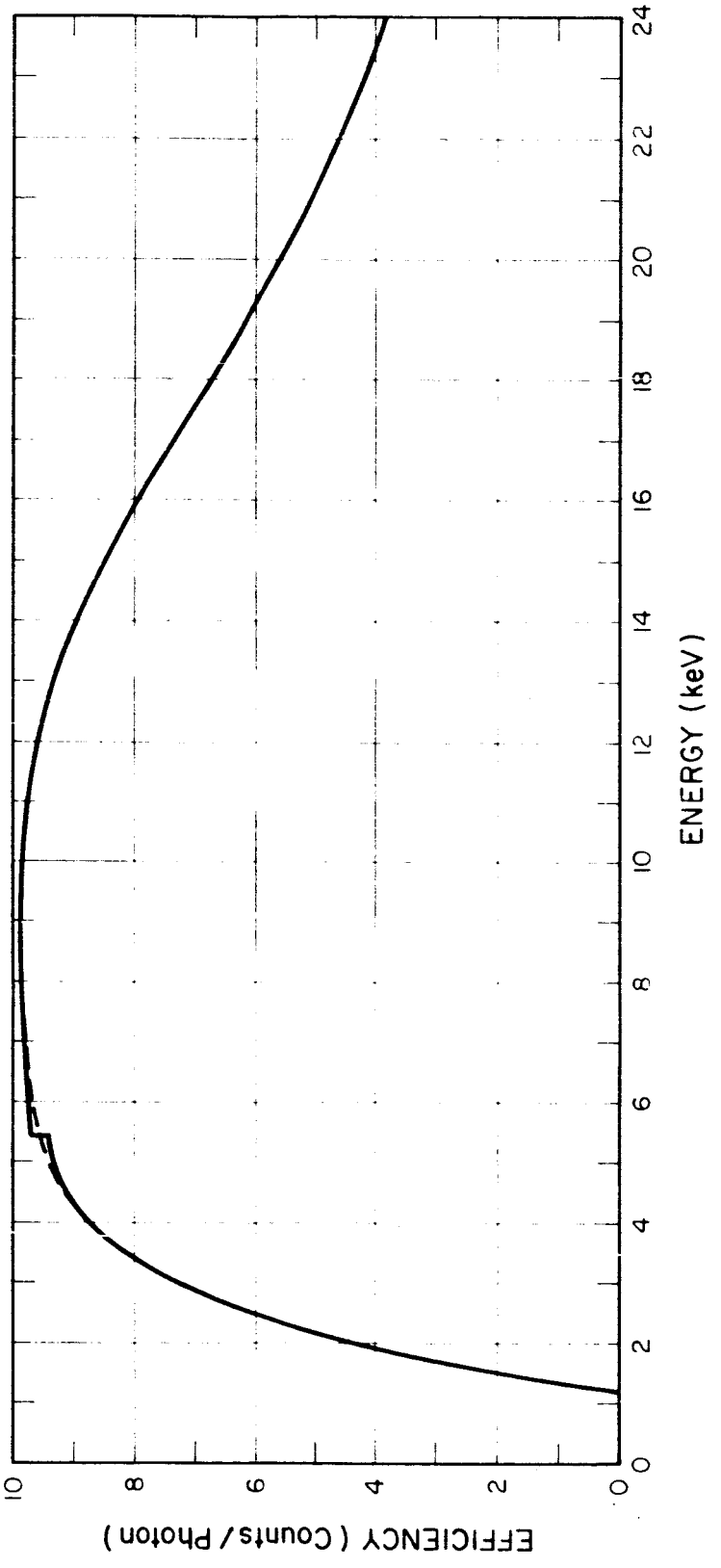

CALCULATED EFFICIENCY OF XENON FILLED COUNTERS

Figure 2

the flux at these low energies. The question of the determination of rocket aspect still remained. In previous flights we had made use of photoelectric star sensors to make this determination. The system was completely successful; indeed, the limit in precision was the instrument survey; namely, the location of the several instruments with respect to each other on the payload. However, the analysis of aspect data and the counter data itself, was made extremely complicated by the high spin rate of the payload. A spin rate of 2 rps is the same as 720°/sec. In order to achieve 0.1° precision, timing measurements must be accurate to about 0.15 ms and it was not clear to what extent this is permitted by the telemetry. The highest bandwidth attainable with the existing Aerobee telemetry systems (this is related also to ground facilities at WSMR) is about 2000 cps; thus, small delays anywhere in the telemetry system can introduce systematic errors in timing and throw off the attitude measurements. It should be noted that the effective bandwidth in an experiment is much larger than the stated specification of the telemetry system because of the fact that the measurement is repetitive. As an example of the complication involved in the data analysis, it was necessary, in previous experiments, to determine the spin period to $1:10^{5}$ in order to superimpose the data obtained during the entire flight.

We considered the possibility of despinning the payload portion of the rocket by making use of a Ball Brothers Research Company despin table. This unit, would be contained in a standard Aerobee extension mounted between the payload and the sunstainer. The despin table operates by counter rotating one portion of the rocket against the other; a rate gyro being used to control the rate of rotation of one portion (in our case the payload) and the remaining portion is free

to take up all the excess angular momentum. The unit is similar to the one utilized in the BBRC biaxial solar pointing control. The principal of operation is that the net angular momentum of the rocket does not change (angular momentum is transferred from one portion to the other); the rocket retains the small amount of precession corresponding to a high spin condition as opposed to a very large precession angle resulting when the net angular momentum of the rocket is reduced to a small value as with a Yo-Yo despin, but the payload can be made to rotate at an arbitrarily slow value. However, the introduction of the despin table causes other complications; namely:

1. Jitter in both the spin direction and the direction normal to the spin. The latter is caused by wobble in the bearings; the former is caused by friction and represents a non-uniform spin rate. Both of these effects have a periodicity corresponding to the net (high) rotation rate of the vehicle.

2. The TM antennas would be mounted near the payload. In previous experiments we had mounted the antennae on the tail. This produced a radiation field on the ground that is more readily detected than the corresponding field produced by antennae mounted at the payload. Also since the antennae are remote from the experiment instruments, there is less of a problem with electrical interference caused by the RF field.

These are both major considerations that could adversely affect the conduct of the experiment and were very difficult to access prior to the actual construction of the payload. Another problem was:

3. The star sensor arrangement used in the previous rocket flights was not directly useable with a despin payload. The reason for this is that the number of star acquisitions per rotation is too small to determine the precession parameters. (We had considered allowing only two rotations of the payload during the flight). Thus we needed an entirely new aspect system based on the use of a camera for photographing the star field.

In view of these considerations and also of the problems associated with the actual procurement and refurbishing of the despin unit, we decided to proceed with the conventional spinning rocket as we had in the past, but making more of an effort to eliminate systematic errors in the aspect determination. Related to this question of systematic errors, was the question of the instantaneous axis of rotation of the rocket; i.e., given the sighting of a sequence of stars along a given great circle, it is generally necessary to extrapolate between two successive star sightings in order to determine aspect at a particular time. This necessitates drawing an arc of a great circle, corresponding to the actual scan line, which necessitates knowing the instantaneous spin axis. In previous experiments, it was assumed that the longitudinal axis of the rocket (the symmetry axis) coincided with the spin axis; however, the rocket will actually spin around one of the principal axes of inertia. It is necessary to spin-balance the entire rocket to determine this axis, such facilities were not available and it was decided to incorporate a star sensor in the payload that would measure its location in flight. This star sensor was mounted in the tip of the rocket and looked out along the nominal spin axis.

A further complication was encountered with respect to the aspect problem, namely, the firing time. In order to achieve the scan of the galactic equator, the rocket needed to be launched at about 13 hours sidereal time. During the time of year for which the rocket was scheduled this necessitated a daytime launch - a four month delay would have been necessary to achieve a night time launch.

The final list of instruments and their function is listed below.

1. Proportional Counters. - 2 mil Beryllium windows, Xenon gas filling. overall dimensions 2 x 2 x 6", sensitive area 36 cm^2. Six counters in two banks.

2. Geiger Counters. 2 mil Beryllium windows, Xenon gas filling, overall dimensions 1 x 2 x 6", sensitive area, 18 cm^2. Twelve counters in two banks.

3. Photoelectric Detector.

4. Star Sensors. One radially mounted, one axially mounted.

5. Sun Sensor.

6. Magnetometers.

The orientation of the detectors is listed in Table I.

TABLE I

ORIENTATION OF INSTRUMENTS

The coordinate system used is one in which elevation is measured from the rocket z axis (the long axis of the rocket, +z being toward the tip), azimuth is measured in the plane normal to the z-axis, with the azimuth of the Geiger counters taken as zero and is measured in a right hand sense around the +z axis. The rocket rotation is in the same sense.

Detector	Azimuth	Elevation	Field of View		(FWHM)
			A z	Elev.	
Upper Geiger counter	0	90°	1.5°	40°	(1)
Lower Geiger counter	0	90°	1.5°	40°	(1)
Lower Star sensor	0	75°	2°	7°	
Upper Sun sensor	0	90°	1.5°	40°	
Lower Sun sensor	0	90°	1.5°	40°	
Upper Star sensor	-	0°	4^{0}	10°	
Photoelectric det.	0°	75°	5°	10°	
Upper prop. counter	180°	90°	2°	40°	(2)
Lower prop. counter	180°	90°	2°	40°	(2)
x-Magnetometer	90°	90°			(3)
y-Magnetometer	180°	90°			(3)

Notes:
1. Modulation collimator
2. Slant collimator
3. +Axis of magnetometer taken as running toward the cable end.

3.0 HARDWARE DESIGN

The payload was a refurbished version of what had been flown on Aerobees 4.122 and 4.123 thus new design was minimal. A certain amount of redesign was inevitable; a new counter configuration was utilized that made more efficient use of the available area which in turn entailed new collimators. One star sensor was renovated and a second star sensor was designed for use in the tip. An ejectable tip was provided in the payload. The use of proportional counters made necessary the incorporation of a low noise preamplifier and modification of existing stretching logic. Individual instruments are described below.

3.1 Geiger Counters

Two banks of six counters each were incorporated in the payload. Each counter was filled with xenon gas and had a beryllium window. The counters were designed to have a threshold 1300 volts and were normally operated between 1400 and 1500 volts. A bank of six counters is shown in Figure 3. The electronics associated with these counters was similar to that used in the previous payloads. A block diagram of the logic is shown in Figure 4. Two separate amplifier, discriminator, straps, channels, are provided; one for the Geiger counter signal, the other for the signal from a veto counter (plastic scintillation counter). Geiger counter signals are not recorded if they are time coincident with the veto signals (linear antigate). Acceptable signals drive a scaler whose output is a staircase function that goes directly to a clear telemetry channel. Other significant features are: 1) if the Geiger counter signal is too large (as might result from arcing) a veto signal is generated and 2) following any Geiger counter signal a 1 ms deadtime is imposed on the circuit. This prevents afterpulsing from being recorded as counts.

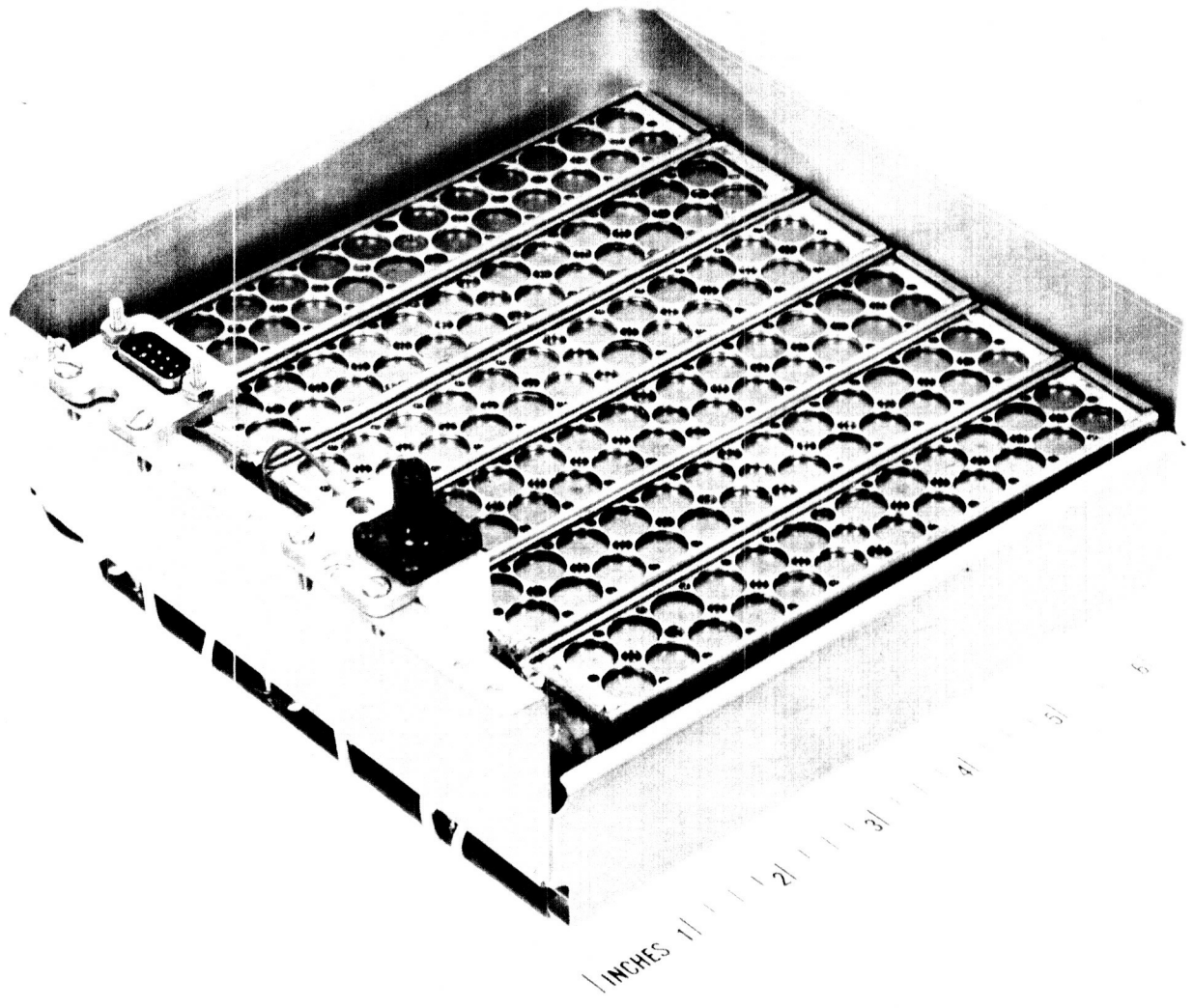

DD-0028

Figure 3

BANK OF GEIGER COUNTERS

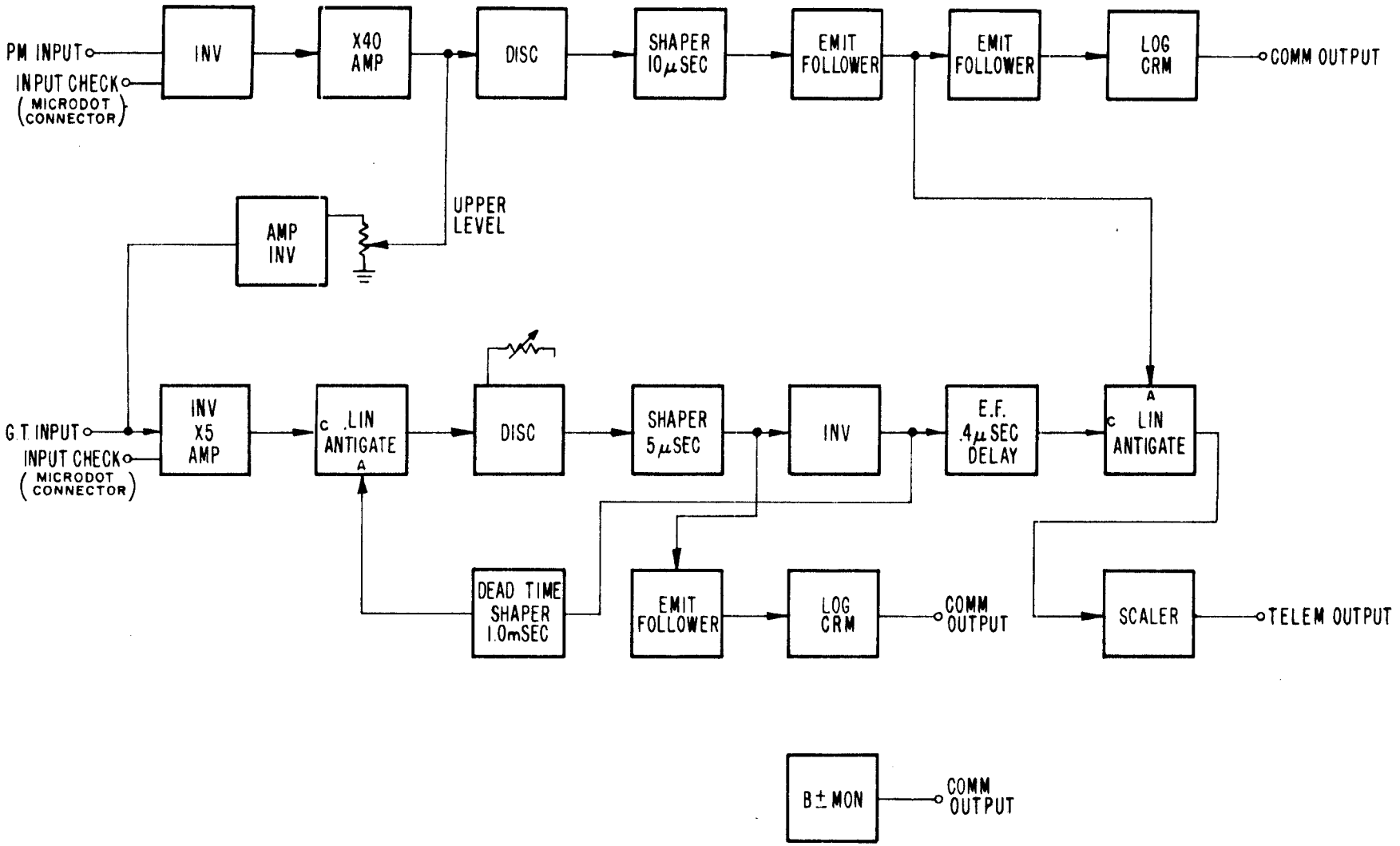

Figure 4

GEIGER TUBE LOGIC

3.2 Proportional Counters

Two banks of three counters each were incorporated in the payload. Except for their size (2 x 2 x 6") those counters were identical to the Geiger counters. A bank of counters is shown in Figure 5. Each counter was provided with a preamplifier that incorporated an automatic cutoff feature to block the output in the pulse rate exceeded a certain pre-set level. A logic diagram of this circuitry is shown in Figure 6. The linear output of the preamplifier went to circuitry identical to what had been used in the previous experiment for the X-ray scintillation counters which consisted of a stretcher that preserved the pulse height of individual signals. The stretched signals were telemetered directly.

3.3 Photoelectric Detector

This device was the identical unit that was used in previous rocket measurements.

3.4 Radial (Lower) Star Sensor

This unit was one of the star sensors developed for the earlier rocket flights. The optics consisted of a 3" f:1 fresnel lens and a single slit in the focal plane. The photomultiplier was an RCA C70129B which is a miniature tube with an internal photocathode. The field of view of the star sensor is shown in Figure 7. The slit was broken in the middle of its field to allow the unambiguous determination of the elevation of a given star at certain times; i.e., a given acquisition of a star determines azimuth elevation is fixed only within the width of the slit. With a spinning, yawing rocket, the same star is observed repeatedly, but, because of the yaw, when the star crosses the scan plane, it disappears. At that instant the elevation of the star is uniquely determined.

3.5 Axial (Upper) Star Sensor

The need for this sensor was previously discussed. An

BANK OF PROPORTIONAL COUNTERS

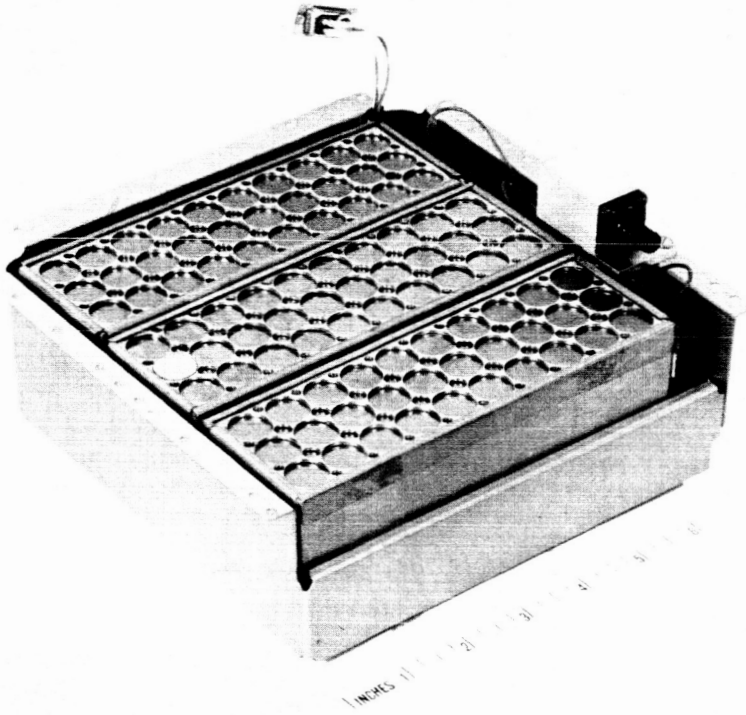

OD-004 FRONT VIEW SHOWING COUNTER FACE

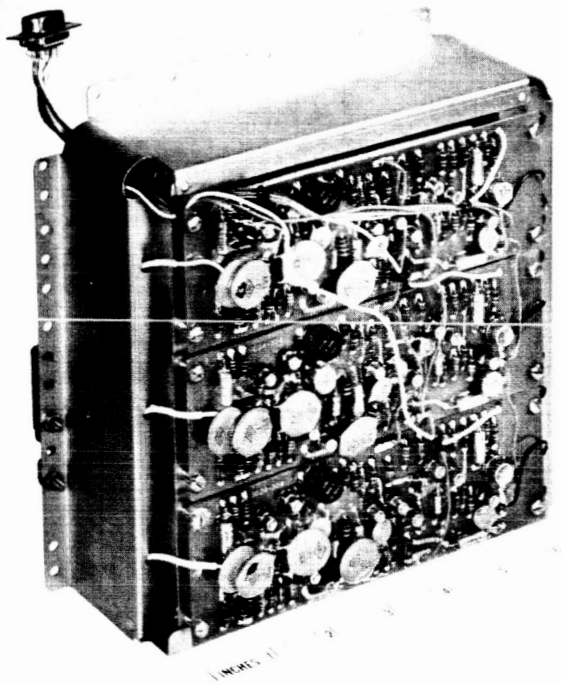

OD-005

REAR VIEW SHOWING PREAMPLIFIERS

Figure 5

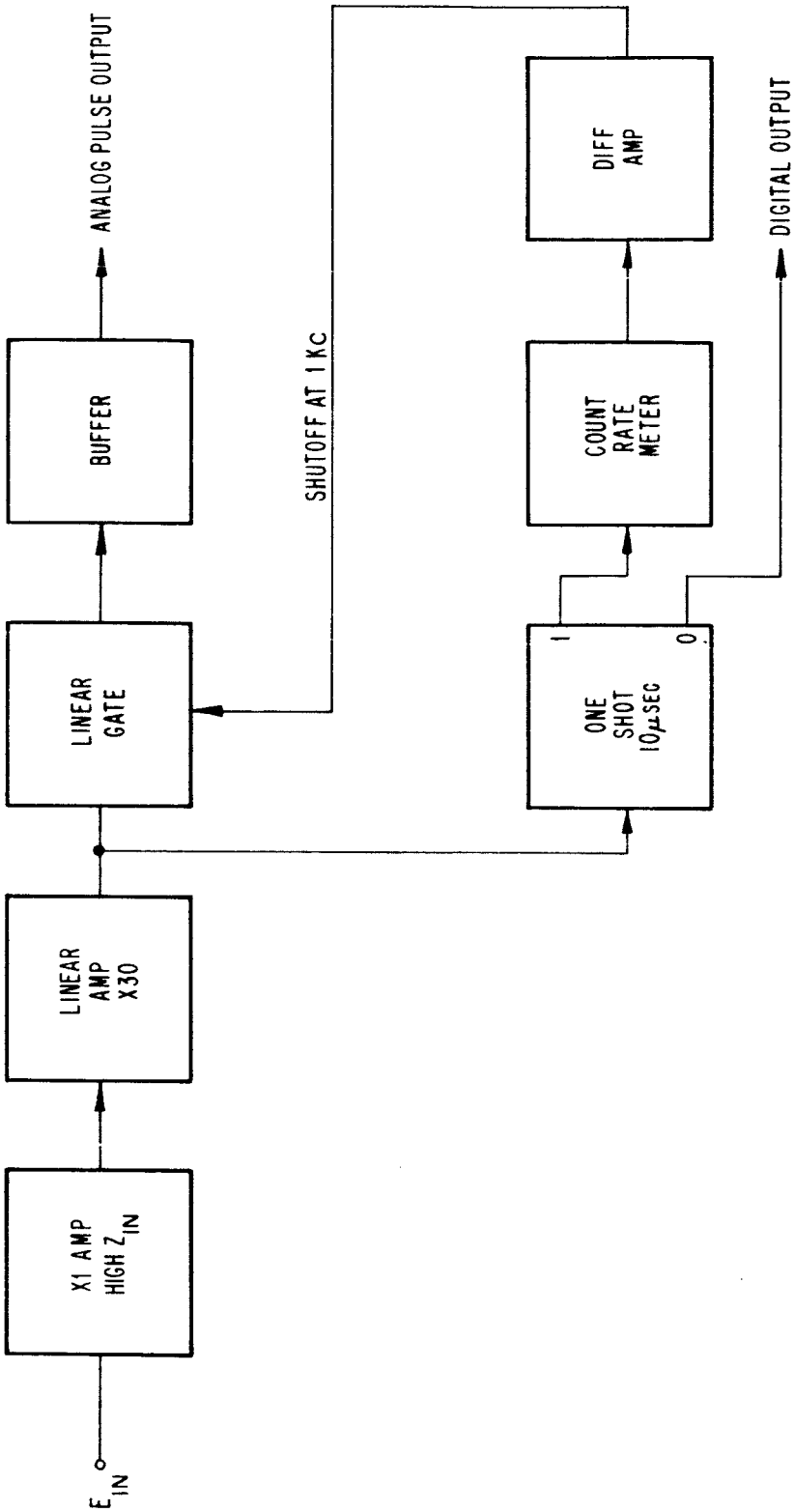

PROPORTIONAL COUNTER PREAMP

Figure 6

STAR SENSOR FIELDS OF VIEW

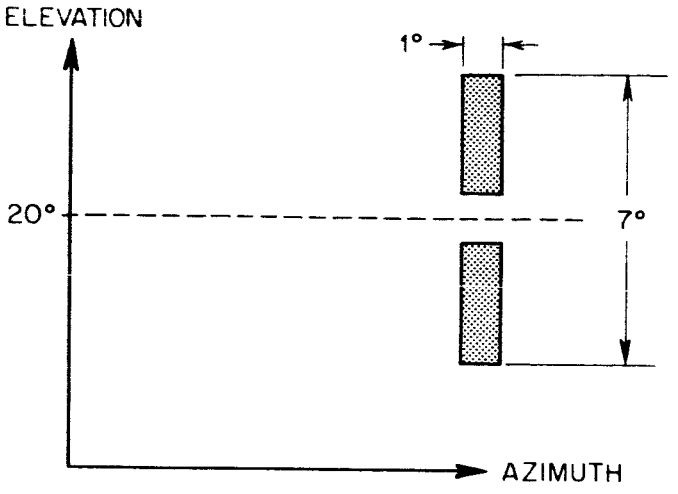

RADIAL SENSOR

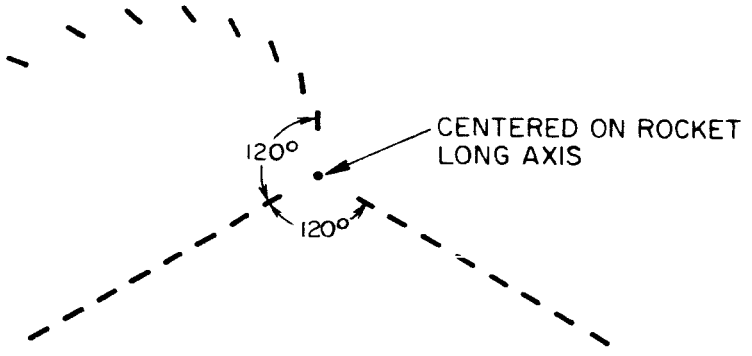

AXIAL SENSOR

Figure 7

entirely new device was developed that incorporated a 2" f:2 Nikon lens and an 1 1/2" diameter, end window photomultiplier (RCA C70114) as the light detector. The use of the large diameter multiplier allowed the incorporation in the focal plane of an extensive slit system as opposed to the single narrow slit utilized in the radial star sensor. The actual slit system used is shown in Figure 7. The center of the slit system is made to coincide with the longitudinal axis of the rocket (in practice, it is defined as that axis). Per rotation a star will traverse each of the three slits, two of the slits are separated in azimuth precisely 120°, the third slit is at a varying azimuth that allows approximate determination of (within 1°) of the elevation of star (the angle from the center). Each slit is broken into 1° segments so that during the precession cycle a star will disappear when it crosses from one segment to the next at the instant of disappearance the elevation of star is precisely determined ($\sim 0.1^{\circ}$). Since the elevation can be determined from each of three slits, it is possible to locate the spin axis with respect to the center of the slit system (longitudinal axis of the rocket).

3.6 Sun Sensors

The sun sensors consisted of solid state photodiodes. The solar radiation was transported to the photodiode by a lucite rod mounted behind the set of collimators that were used in conjunction with the Geiger counters.

3.7 Magnetometers

The magnetometers were Schoensted Model RAM 3C units. Two were used in the payload; both were mounted radially.

3.8 Collimators

Collimators were used in front of the proportional counters and the Geiger counters in order to limit the acceptance directions of the X-rays. Slat collimators were used in conjunction with the proportional

SLANT COLLIMATORS

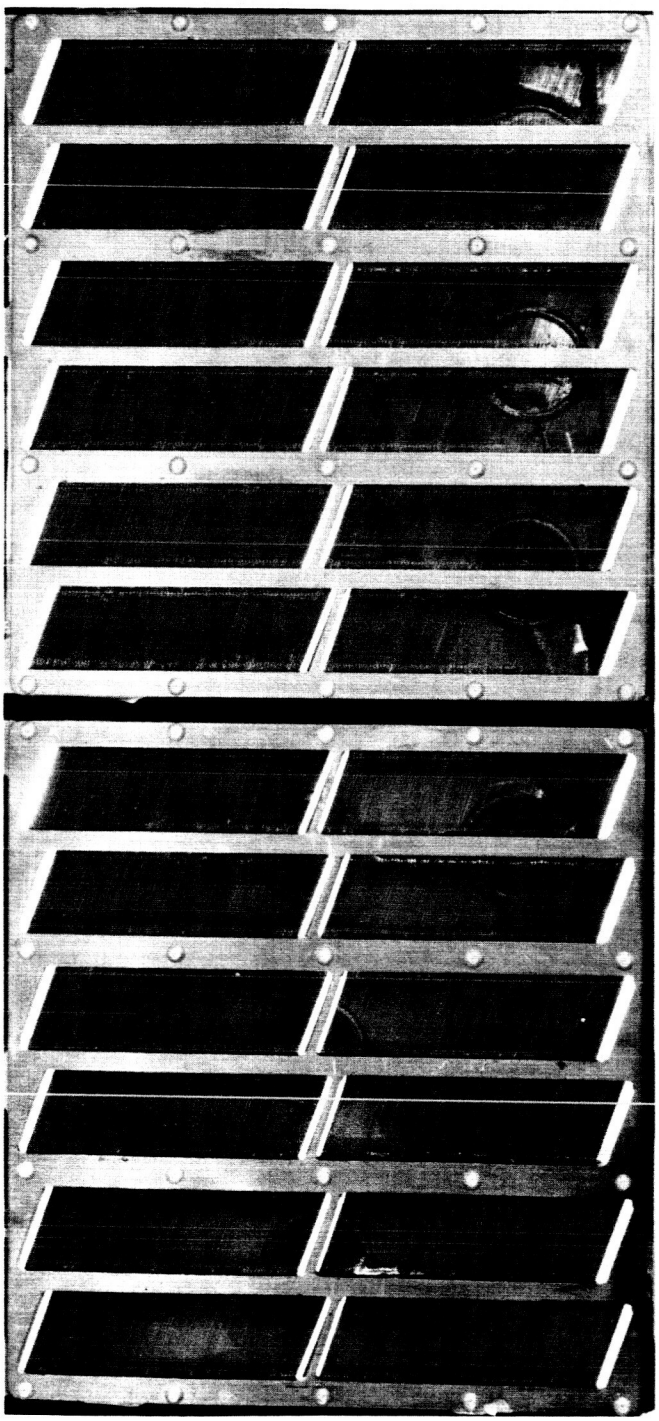

DD-008

Figure 8

collimators. The slats were fabricated from 0.01" stainless steel and individual slats were separated by 0.03". The field of view of the collimators was nominally 2^{o} x 40^{o} full width at half maximum. An assembled collimator is shown in Figure 8. The slats were slanted by 30^{o} to the scan plane, which meant that the azimuth at which a source would be observable was a function of the angle of the source off the scan plane.

A combination modulation collimator and slat collimator was used in conjunction with the Geiger counters. The slat collimator was similar to that used with the proportional counter except that it was not slanted with respect to the scan plane. The field of view was 1.5^{o} x 40^{o} (FWHM). The modulation collimator consisted of electroformed grids spaced 2" apart. An individual grid is shown in Figure 9. The grid wires were 0.0025" in diameter and spaced on 0.005" centers. With the 2" spacing between grids this yielded a collimator whose angular resolution was 8 arc minutes. The effect of the modulation collimator was to break the 1.5 x 40^{o} field of view into a series of parallel bands separated by 8 arc minutes. The direction of the bands was parallel to the scan plane.

3.9 Assembly

The overall rocket is shown in Figure 10. The basic structure was not significantly modified from the unit utilized in the previous rockets. The star sensors and magnetometers were remounted, the housekeeping unit and the photoelectric detectors were unchanged. The counters and collimator assemblies were new, but were mounted in the same veto-scintillation counter as in the previous payloads.

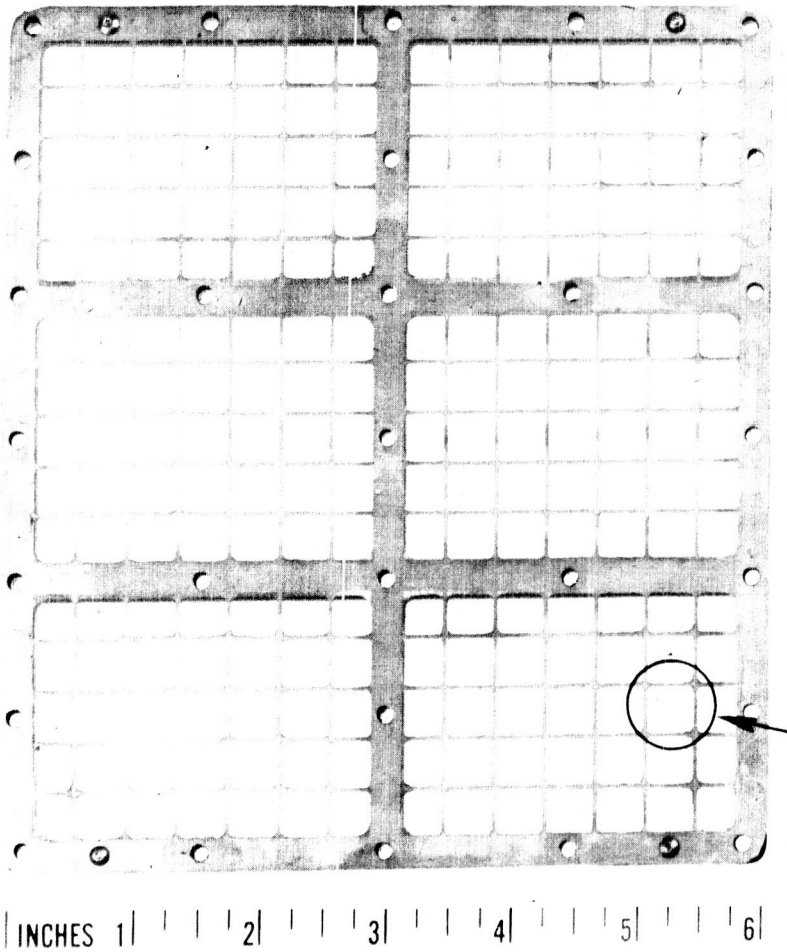

DE-022

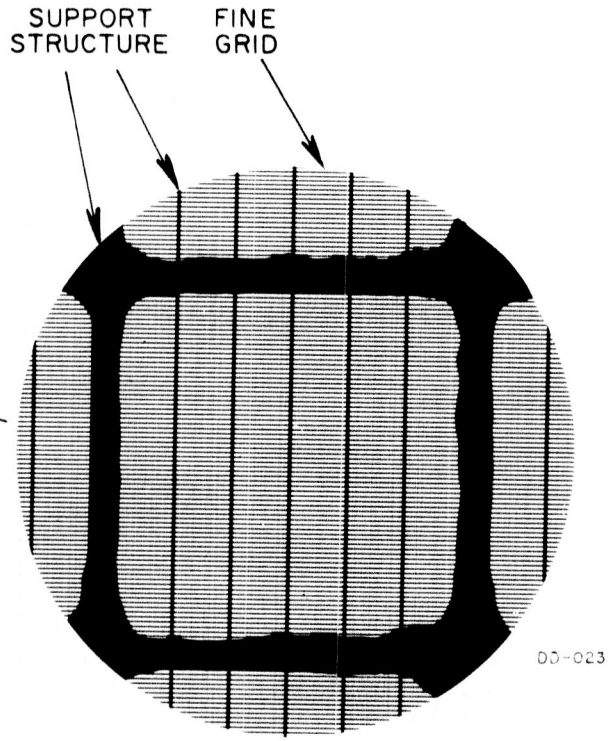

DD-023

Figure 6

SINGLE GRID USED IN HIGH RESOLUTION MODULATION COLLIMATOR

ASSEMBLED PAYLOAD FOR NASA 4.147

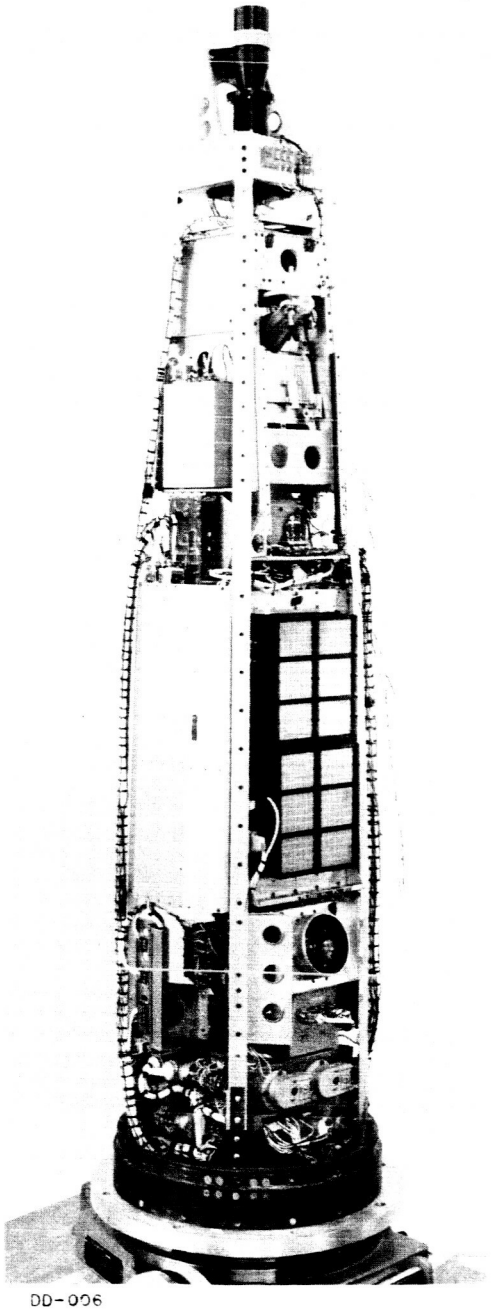

DD-006

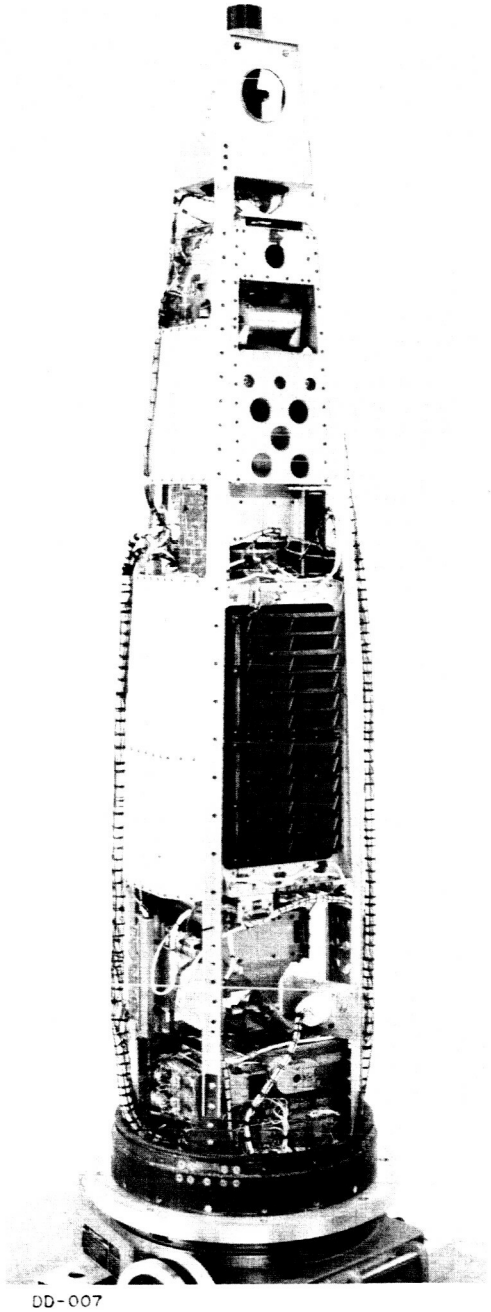

DD-007

Figure 10

4.0 TESTING AND CALIBRATIONS

Work was initiated on preparing the payload for flight during May 1965. All fabrication was completed by the last week in July and a fully assembled payload was available by 9 August. From that time the following schedule of operations was adhered to:

9 August	-	Systems testing of payload
16 August	-	Vibration testing
		Vacuum testing
23 August	-	Payload integration at GSFC
30 August	-	Instrument alignment at AS&E
7 September	-	Arrival at WSMR
15 September	-	Launch date

Prior to 9 August there had been extensive testing of individual sub-assemblies. These included thermal (from 0°c to 40°c) testing of all electronic assemblies, vacuum testing of all assemblies that involved high voltages. Equipment was left on during the entire vacuum test to assure that no damage could be incurred in going through the corona region. During the flight,with the exception of the photoelectric detector, all high voltages were on at launch. The high voltage for the photoelectric detector was switched on at about 100 seconds into the flight. Additional testing included routine calibrations of the various input functions versus the telemetry output.

Two sub-assemblies, the X-ray counters and the star sensors, were subjected to much more extensive testing than the others. The counters, both Geiger counters and proportional counters, were vacuum cycled upon delivery and several times during the program. The properties of the counters were measured on a weekly basis. For the Geiger counters this consisted of measuring the plateau curve (counting rate as high voltage) and for the

the resolution at several X-ray energies. Figure 11 shows the proportional counter response to X-rays at 1.5 kev produced by a continuous X-ray spectrum filtered by aluminum.

The star sensors were tested for their sensitivity to starlight and to bright light transients. The latter was of particular importance because of the fact that the rocket flight was planned for daytime. Figure 12 shows the response of both the star sensors to very bright light and indicates that for both recovery was complete within about 50 milliseconds following the end of the light pulse.

The relative alignment of the several instruments represented a major problem because of the attempt to achieve ultimately a precision of better than $1/4^{\circ}$ in location; the problem being that the X-ray detectors and star sensors are separated on the payload. The entire alignment was performed using visible light, separate measurements had established that the direction of maximum transmission of the X-ray collimators in visible light was the same as in X-rays. The alignment was measured in two different ways. In the first, the rocket was set up vertical on a rotary table (see Figure 13), a 6 inch reflecting telescope was used to provide a collimator beam of light whose divergence was less than 1'. The telescope was attached to a rotary table that allowed rotation of the telescope in a vertical plane. The combination rotary table-telescope was mounted on a milling machine that allowed about 24 inch excursion in both vertical and horizontal directions. The rotary tables allowed measurement of angles to within several arc minutes. The milling machine allowed transporting the telescope (ie: the collimator beam of light) without changing its direction by more than 1'. With this set up, the relative orientation of the several X-ray collimators and the radial star sensor was determined by mapping the response to the collimated light beam.

RESPONSE OF PROPORTIONAL COUNTERS TO THICK TARGET BREMSSTRAHLUNG

4.0 keV +1mil ALUMINUM

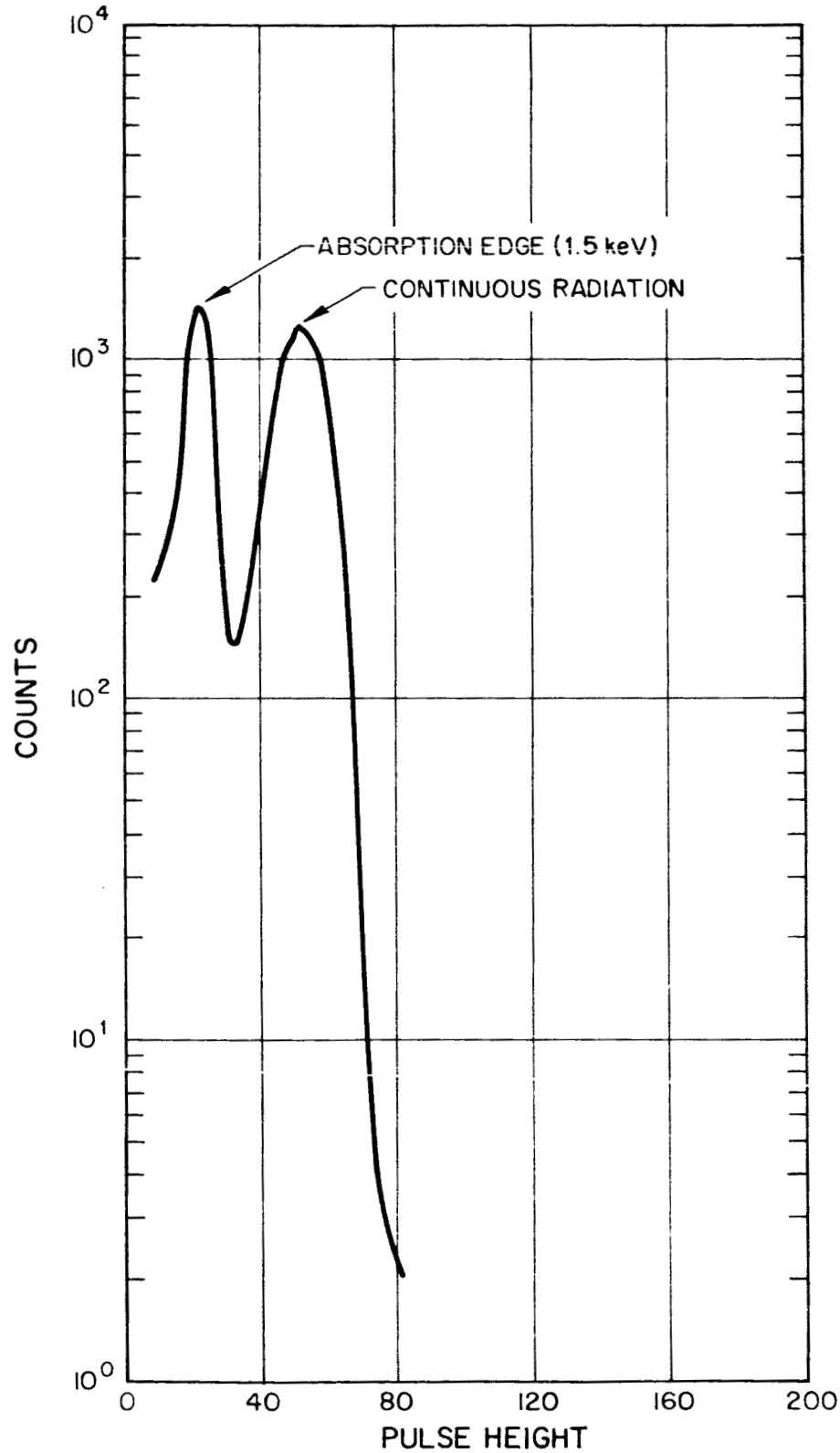

Figure 11

1372

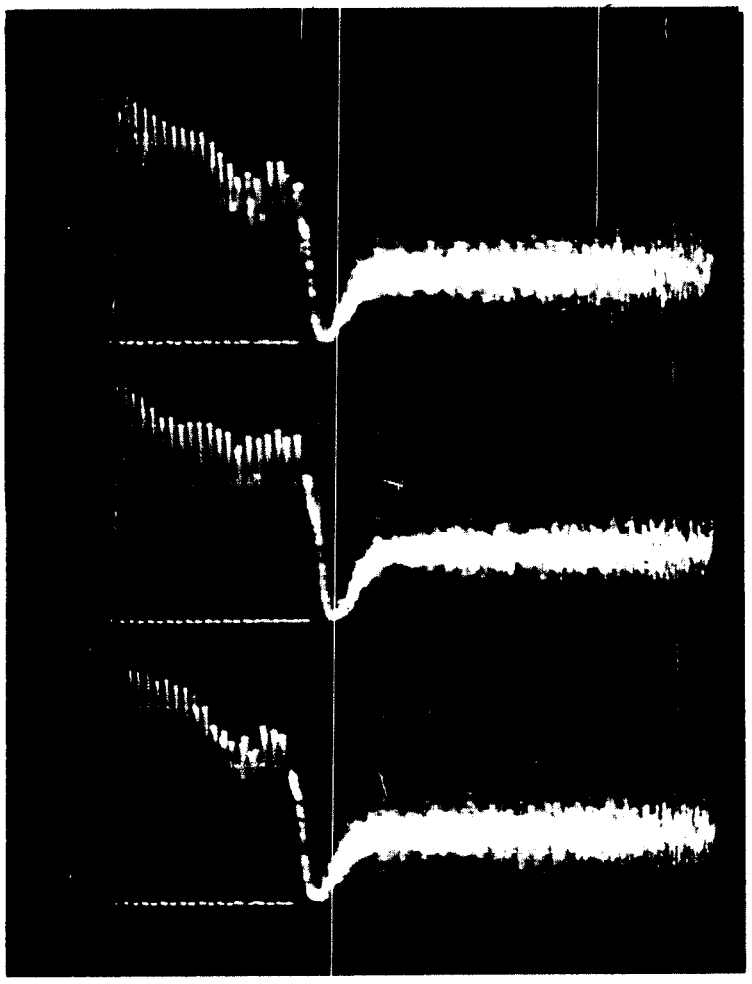

DD-083

AXIAL STAR SENSOR

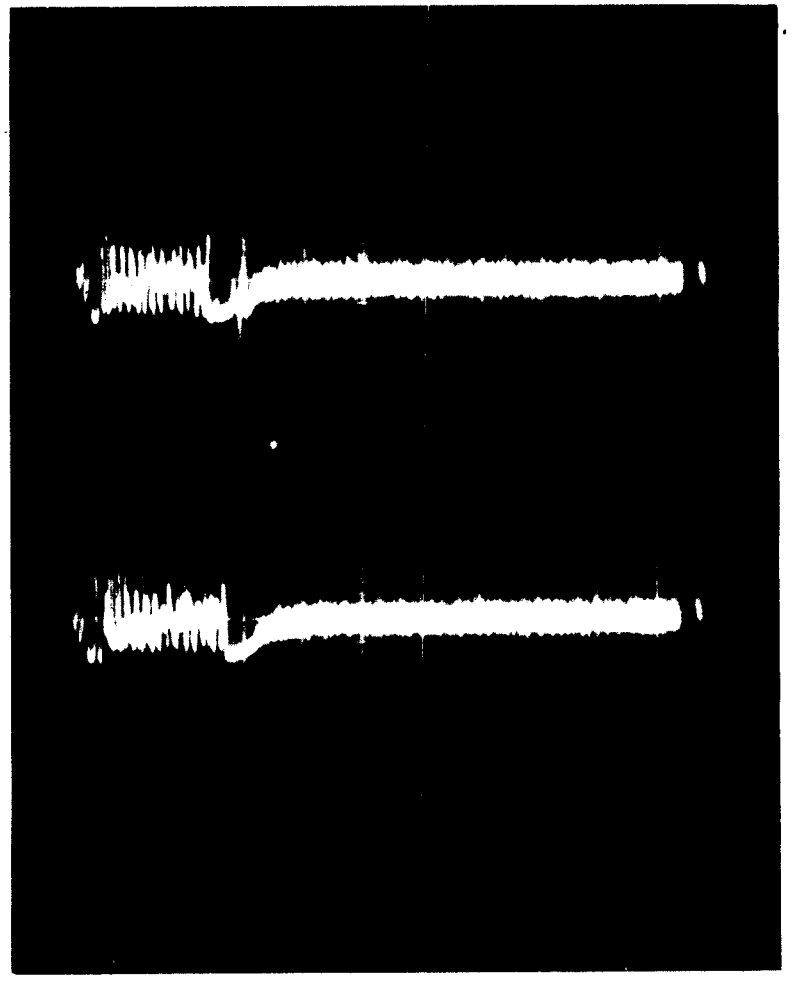

DD-084

RADIAL STAR SENSOR

RESPONSE OF STAR SENSORS TO BRIGHT LIGHT IMPULSES

SWEEP TIME = 50 m sec/cm DEFLECTION = 1 volt/cm

Figure 12

The orientation was measured with the telescope inclined at many different angles. In the second arrangement, the rocket payload was made horizontal and the orientation was measured with a pair of theodilites. The theodilites were used to sight on the several detectors; in the case of the star sensors, the theodilites were focussed to infinity and viewed the slit in front of the photomultiplier through the sensor optics. For each measurement orientation, a four sided figure was determined with the two theodilites, the axial star sensor and another detector forming the corners of the figure. Using the angles defined by the theodilites at their respective corners, the angle between the two detectors on the payload could be determined.

MEASUREMENT OF ALIGNMENT

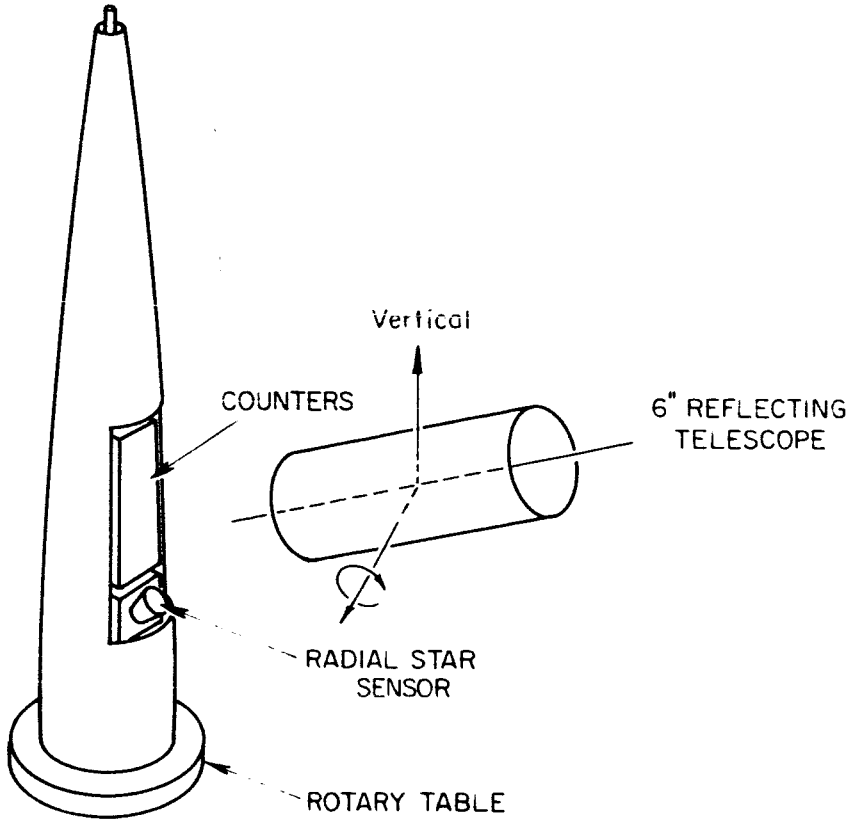

VERTICAL ALIGNMENT PROCEDURE

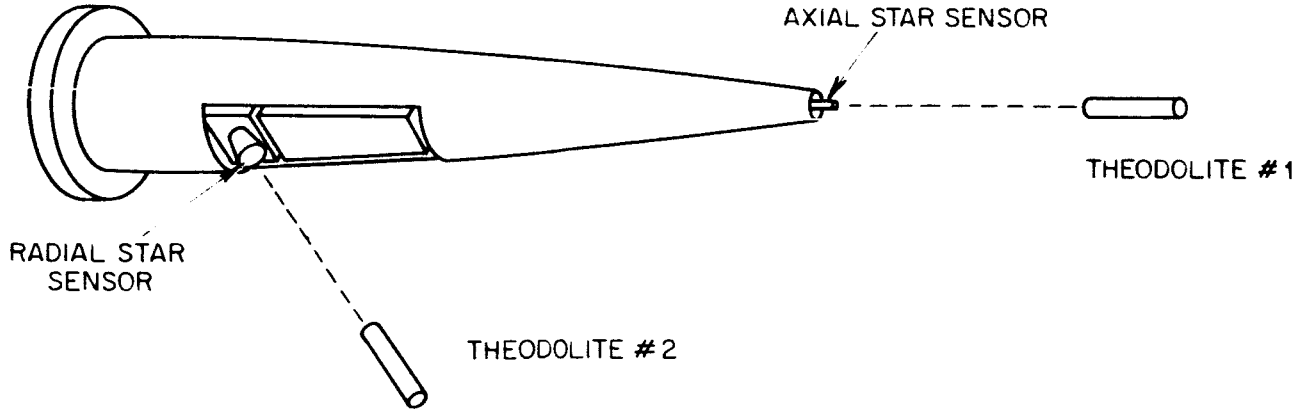

HORIZONTAL ALIGNMENT PROCEDURE

Figure 13

5.0 FLIGHT - 4.147

Following successful completion of integration at GSFC and final calibration and alignment at AS&E, the payload was shipped to WSMR. The following was the schedule of operations carried out at WSMR.

7 September 1965		Rocket available
9 September 1965	AM	Pre-flight conference
9 September 1965	PM	Horizontal Instrumentation check
10 September 1965	AM	Weigh and set fins
10 September 1965	PM	Vehicle in tower
13 September 1965	PM	Vertical Instrumentation check
15 September 1965		Launch

The rocket had been originally scheduled for launch on 15 September 1965. A misfire occurred and forced a cancellation of the flight. The flight was rescheduled on the next earliest date that the range would support a launch; namely, 22 September. The nature of the misfire was failure of the booster to ignite. There was no apparent damage to the payload. The rocket was successfully launched at 13:07 MST on 22 September 1965. The flight was as predicted and the rocket reached a peak altitude of 124 miles. Telemetry data was received from all instruments for a total of 395 seconds; of this, 315 seconds was during the portion of the flight that the rocket was above 80 km. The parachute recovery of the payload was not completely successful. Upon impact, the front portion (12") of the payload and ogive were crushed. The force of the impact sheared sixteen #10 steel screws that held the payload to a base ring. The recovered payload is shown in Figure 14.

RECOVERED PAYLOAD

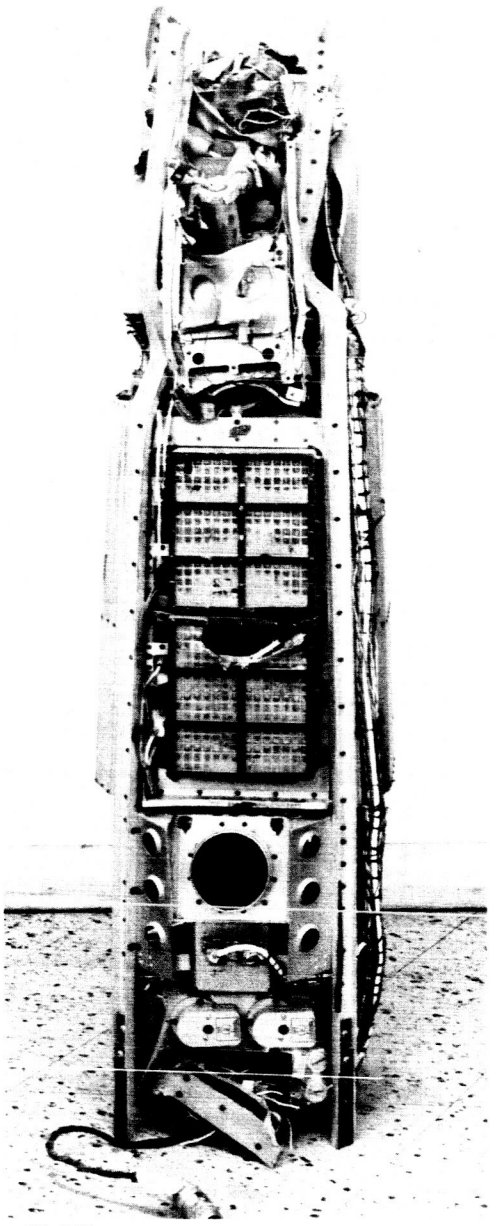

DD-020

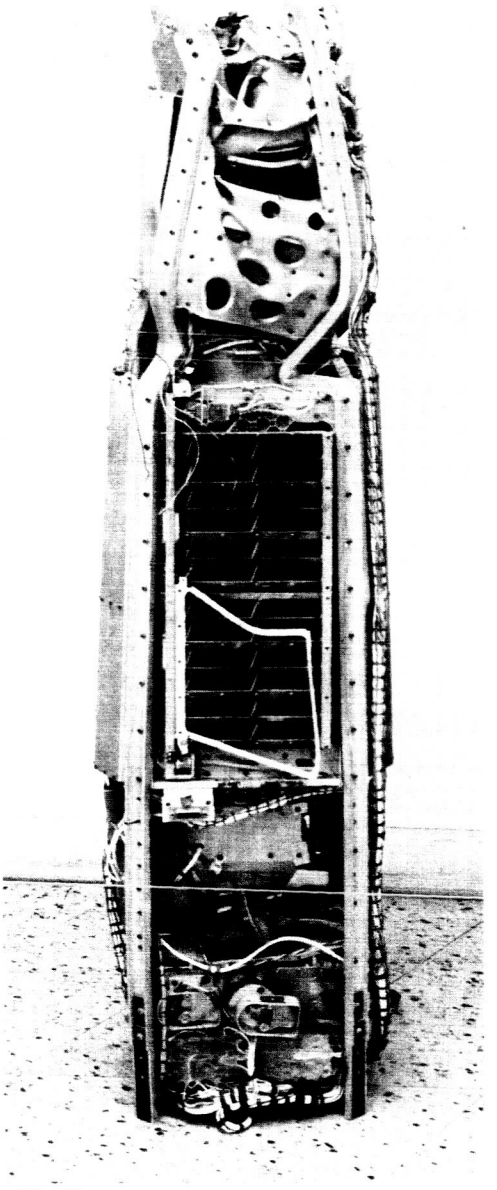

DD-021

Figure 14

The bulk of the instrumentation worked as expected. One significant failure occurred; the door to the photoelectric detector failed to open. The Geiger counters and proportional counters were functioning at launch and there did not appear to have been any failure in their operation.

6.0 PRELIMINARY DATA ANALYSIS

In spite of the apparent success of this rocket flight and the recovery of the bulk of the telemetered data, it has not proven possible to extract much useful information on the basis of preliminary analysis.

A superposition of the data obtained from one of the detectors is shown in Figure 15, which indicates the existence of only a single X-ray source. A number of circumstances have complicated the analysis of these data. These are:

1. A higher (3 rps) than anticipated spin period.
2. Poor aspect data. Stray sunlight makes it difficult to pick out stars.
3. High background in the X-ray counters.

The background counting rate was about 1 ct/cm^2 -sec, which was about three times higher than had been previously observed. This background radiation was not soft (< 10 kev) since it did not show any altitude variation. The higher background than had been previously observed can apparently be accounted for by the change to Xenon filled counters as opposed to Argon filled counters that we had previously employed. The efficiency of the Xenon counters extends to well above its K-edge at 32 kev.and is about 100 times more sensitive to the local (produced in the Earth's atmosphere by the cosmic rays) γ-ray background than are the same counters filled with Argon.

It does not appear that we yet have the correct superposition of the data. The single peak observed in Figure 15 has a width of 12^o which is about three to four times the angular width of the collimators. Of course,

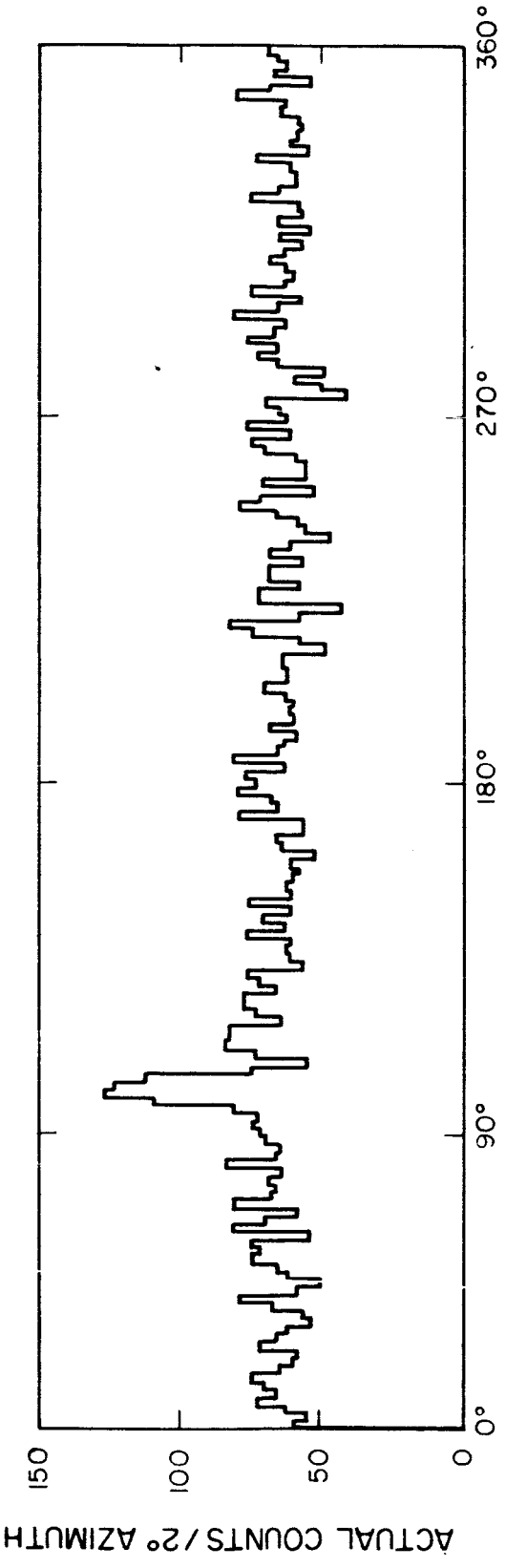

AZIMUTHAL DISTRIBUTION OF COUNTS
LOWER PROPORTIONAL COUNTER

Figure 15

if the same number of counts is concentrated in a narrower peak, the signal to noise ratio improves correspondingly, and it could be that additional sources will appear in the data when the data can be superimposed correctly.

7.0 EXPERIMENT PLAN 4.148

The experiment plan for rocket 4.148 was conceived during the summer of 1965, prior to the flight of Aerobee 4.147. The experiment, from an instrumentation point of view, was to represent a radical departure from previous ones. The rocket was to be ACS equipped which permitted scanning over limited regions of the sky or even restricting the entire observational time to a single X-ray source.

Before discussing the actual experiment it is useful to review the observational status of X-ray astronomy as of that time.

1. ScoX-1, the brightest known X-ray source, was located 25° from the galactic equator. The X-ray flux, in the range of 1-10 kev, was about 10^{-7} ergs $-cm^{2}-sec$. There was no apparent visible or radio counterpart.

2. A group of sources were clustered near the galactic center and within several degrees of the galactic equator.

3. Isolated sources had been observed along the galactic equator in Cygnus, Serpens and Taurus.

4. The source in Taurus was apparently the Crab Nebula. The angular size of the X-ray emission region was finite (1 to 2 arc minutes). This was the only source with a known visible or radio counterpart. The theoretical status os X-ray astronomy was such as to offer little help to the experimenter. The neutron star hypothesis was in disfavor; first, because the measurement of the angular size of the source in the Crab Nebula is not compatible with a neutron star; and secondly, calculations indicated that the cooling times of neutrons stars would be very short. There still remained synchrotron emission and electron bremsstrahlung as possible X-ray production mechanisms. The latter

tended to be favored (in the form of a hot plasma) but only because it was difficult to construct a model for synchrotron emission that allowed for the continuous and rapid acceleration of very high energy electrons. There was no observational basis for a distinction between the two processes. Although a number of models had been suggested, there was still no satisfying explanation for what was the configuration of matter that could give rise to an X-ray source and how it evolved.

The answers to these questions are clearly the central problem in X-ray astronomy, however, it was also clear to us that the answers probably could not come from observations in X-rays alone. The reason for this is the combined difficulties of first, any space borne experiment; and second, any X-ray experiment. The total observational time available to all experimenters is no more than about 10-15 minutes/year from above the atmosphere. Thus we felt that the most significant experiment that could be performed was the precise localization of an X-ray source to allow ground based astronomers to find and observe the source at leisure. A corollary experiment to measuring location, is the determination of angular size which allows some statement as to what to expect in visible light.

It was also clear that ScoX-1 should be the primary target. The sources near the galactic center are probably obscured by dust and not observable in visible light. Excluding the Crab, the remaining isolated sources were not seriously considered as targets because; first, their intensity was, at most, 0.1 of ScoX-1, and secondly it was not apparent whether more than a single object could be observed during one rocket flight.

We had already been able to make certain definite statements regarding ScoX-1 in visible light. The observed power in X-rays, 10^{-7} ergs -cm^2-sec corresponds to a flux density of 10^{-25} ergs -cm^2-sec (c/s). Provided the source is not optically thick (neutron star) the flux density must equal or exceed this figure in visible light and radio. In visible light this corresponds

to an integrated power of about 10^{-10} ergs $-cm^2$ which is equivalent to a +13 magnitude object. This should be a fairly obvious object in visible light especially if it had possessed finite size. If the source size were too large, the surface brightness would be below observational limits. Taking that limit as +23 m per $(\text{arc second})^2$ meant that the source should be observable provided its angular size was less than between 2 and 3 arc minutes. We had previously established that the angular size of the source was less than 7 arc minutes, and furthermore, we knew from an examination of survey photographs of the region near ScoX-1 that there was no extended object present of the requisite brightness. This left only two possibilities; first, that the angular size was very small and the image was starlike; and, two, the angular size was between 2 and 7 arc minutes. These considerations are of course based on the assumption that a visible counterpart did in fact exist.

We had available an outstanding instrument with which to perform this observation, namely the modulation collimator as originally conceived by Prof. Minoru Oda, along with subsequent innovations notably the inclusion of intermediate grids and the vernier technique. The experiment was thus to consist of measuring the location and angular size of ScoX-1 with the highest possible precision allowable from this combination of X-ray instrumentation, optical aspect system and rocket control. As an auxilliary experiment we included the Crab Nebula as a target during the flight because, 1) it would provide a measure of the capability of the experiment to yield high precision data and, 2) the Crab is of such intrinsic astrophysical importance that any opportunity to obtain new data on that object could not be ignored. The details of this actual experiment are given in Appendix II, which is a paper prepared by Minoru Oda and Herbert Gursky for publication. Appendix II also contains a description of the instrumentation employed in the payload.

8.0 HARDWARE DESIGN

The experiment planned for vehicle 4.148 involved a totally new payload from what had been previously employed by AS&E in its rocket experiments. The basic criteria that evolved as guides in the hardware design were as follows:

1. Use of the cone-cylinder payload configuration to achieve maximum volume;

2. View angle along the roll axis to maximize available length for X-ray collimator;

3. Payload structure of sufficient rigidity to assure stability of the collimator properties;

4. Use of a star photography to determine aspect.

The layout of the instruments is shown schematically in Figure 8 of Appendix II. The instrumentation comprised the payload cylinder, the tip ejection mechanism, the modulation collimators, the proportional counter detectors, the aspect camera, the housekeeping unit and the associated electronics.

8.1 Aspect Camera

The central question in the design of the aspect camera was the sensitivity to stars under the conditions of the flight, and the resolution that could be attained on the film. We conducted a series of ground tests to determine film sensitivity. Figure 16 shows the streaked image of α U maj. (2.0 magnitudes) on Tri-X film while the camera was planning at 1° and 4°/sec. The camera lens was a 50 mm Cooke, fl.4. The observation of other stars on the same photographs indicated that 4.0 mag. stars could be observed at scan rates of 1°/sec. Since we anticipated scan rates of only several arc minutes/second, the sensitivity under flight conditions was estimated to be to stars between 6 and 7 mag. The resolution of this camera for stars is shown in Figure 17 which shows the images of the stars Castor and Pollux under conditions close to minimum sensitivity for detecting a star image. The size of the image is about 20 microns. With a 50 mm focal length lens, this image size, represents an angle of slightly more than 1'; the centroid of the image can be determined to a fraction of this, barring random shifts on the film. We used an estar base film to minimize the effects of film shrinkage and stretching. The field of view of the lens when mounted in the payload was about $3 \times 10^{\circ}$ or 30 sq. deg. The density of 7th magnitude stars is about 0.25/sq. deg which means on the average, several stars would appear in the photograph.

APPEARANCE OF STAR IMAGES WHILE PANNING
(α URSA MAJOR)

4°/SEC

1°/SEC

Figure 16

IMAGE OF INDIVIDUAL STARS

(1/47 SEC FIXED EXPOSURE)

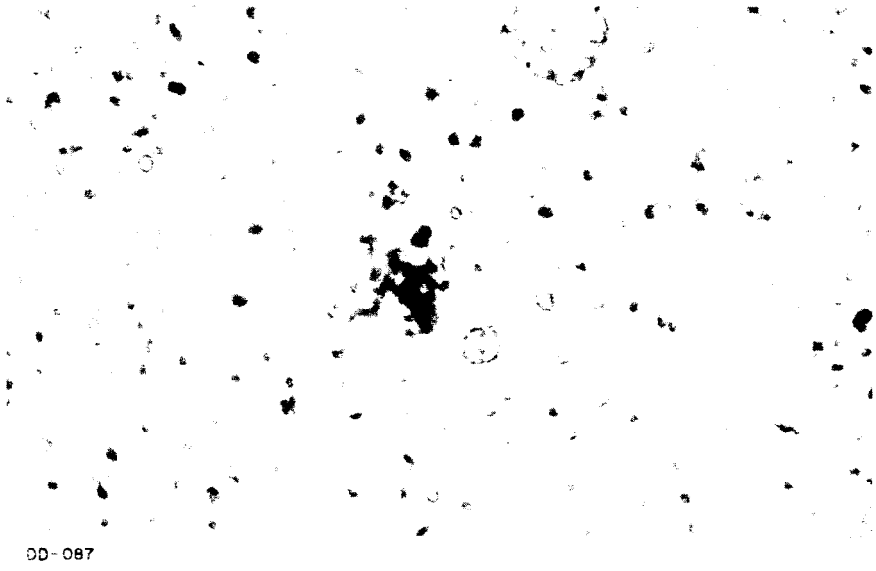

DD-087

CASTOR

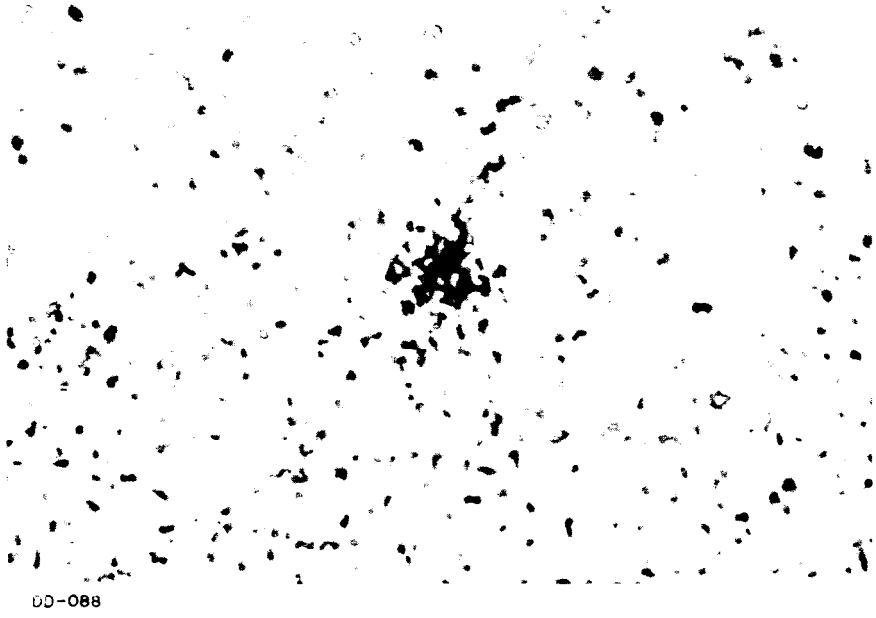

DD-088

POLLUX

Figure 17

8.2 Proportional Counters

The proportional counters were Xenon filled with 9 mg/cm^2 Beryllium windows. Except for dimensions, they were identical to the counters used in payload flown on Aerobee 4.147. The electronics used with the counters was similar to that previously employed; the preamplifiers were identical, but the logic shown in Figure 18 was modified to allow scaling of the output of each counter. Ten counters were incorporated in the payload. The signal output was split in two groups of two counters and three counters for the purpose of telemetering the pulse height information. In addition, the output of each counter was telemetered directly in the form of a staircase (4 steps) function.

8.3 Modulation Collimator

A pair of modulation collimators in a common housing was incorporated in the payload. The two collimators differed by about 5% in their overall length which resulted in a corresponding difference in the angular spacing of their transmission bands. This allowed, by use of a vernier technique, a substantial reduction in the degree of ambiguity that normally accompanies the use of the modulation collimator to measure location. The half-width of each of the transmission bands was about 40", and the separation between bands was about 5'.

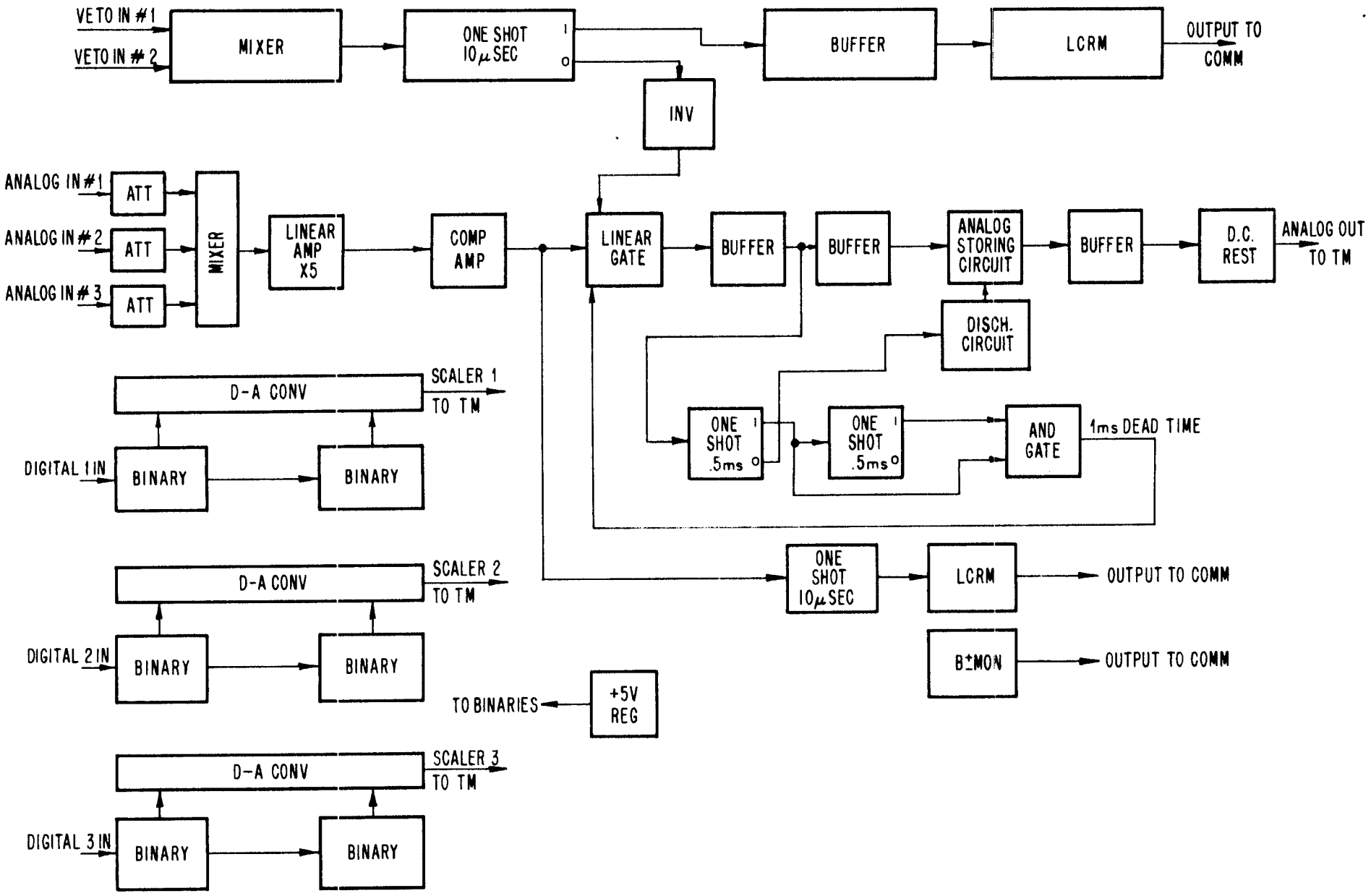

Figure 18

PROPORTIONAL COUNTER LOGIC

8.4 ACS Manuevers

The rocket to be used for this experiment was to be equipped with the standard Aerojet-General ACS package as modified by the sounding Rocket Branch of the GSFC. The manuevers formulated for the ACS are listed in Table II. Ledex position refers to position on a stepping switch that controlled the ACS function. Through position 9, the manuevers are standard for any given flight; they entail bringing the rocket axes to a predetermined orientation which is normally one in which the roll axis is close to local vertical and the pitch and yaw axes are $\pm 45^{\circ}$ off the North-South line. Manuevers 10 and 11 were intended to bring the rocket roll axis (nominally the optic axis of the AS&E instruments) onto the Crab Nebula; position 14 was a roll around the Crab position; 17, 18 brought the roll axis to ScoX-1; and position 21 was a roll around that object. The roll manuevers were necessary to allow measurement along different lines through the source. In this way two dimensional information could be obtained regarding the two target sources even though the modulation collimator is only a one dimensional device. The rocket was to be launched at a time when both objects were approximately equidistant above the local horizon.

8.5 Telemetry Layout

Two telemetry transmitters were incorporated in the payload and the information carried on the various subcarrier channels is listed in Table III. Besides the proportional counter data (PHA a - d, counters 1 - 10) two channels carried information pertaining to timing of the camera operation (Fiducial light #1 and one second clock), five channels contained information regarding the ACS operation and two channels contained AS&E housekeeping data on commutated channels.

TABLE II
ACS COMMAND

The ACS manuevers were as follows:

Ledex Position	Maneuvers
3	Despin
4	Erection
5	Hold
6	Roll Remote Adj.
7	Pitch Remote Adj.
8	Yaw Remote Adj.
9	Hold
10	Roll -25.2°
11	Pitch -80° (to Crab Nebula)
12 - 13	Hold
14	Roll -65°
15 - 16	Hold
17 - 18	Yaw -160.2 (to ScoX-1)
19 - 20	Hold
21	Roll -90°
22	Wait

TABLE III

TM LAYOUT

234 mc transmitter

Sub Carrier	Data
70 Kc	PHA b
52.5 Kc	PHA c
40 Kc	Counter #2
30 Kc	Counter #1
22 Kc	Counter #6
14.5 Kc	ACS Yaw Jet
10.5 Kc	ACS Pitch Jet
7.35 Kc	Commutator AS&E #1
5.4 Kc	Counter #7
3.9 Kc	Counter #5
3.0 Kc	Fiducial light #1
2.3 Kc	ACS Roll Jet

248 mc transmitter

Sub Carrier	Data
70 Kc	PHA d
52.5 Kc	PHA a
40 Kc	Counter #4
30 Kc	One Sec. clock (nominal)
22 Kc	Counter #3
14.5 Kc	Commutator - ACS
10.5 Kc	ACS Yaw Rate
7.35 Kc	Commutator AS&E #2
5.4 Kc	Counter #8
3.9 Kc	Counter #9
3.0 Kc	Counter #10

PHA a consisted of counters 1 and 2, PHA b of counters 3 and 4, PHA c of counters 5, 6, 7, PHA d of counters 8, 9, 10. Counters number 1, 2, 5, 6, 7 were below the long collimator and counters number 3, 4, 8, 9, 10 were below the short collimator. Fiducial light #1 is on the long collimator.

9.0 TESTING AND CALIBRATION

9.1 System Testing

The testing program undertaken for this payload was similar to the one described in Section 4 and Appendix III. Only one serious defect was revealed during the testing; namely the failure of the electro-formed grids of the modulation collimators to withstand vibration. These grids were similar to the ones that had been successfully used in Rocket 4.147, and the failure here was attributed to a difference in mounting (on 4.148, the thrust axis was normal to the grids) and a higher vibration level caused by amplification in the structure. We replaced the electro-formed grids with wire wound grids (shown in Figure 4 of Appendix II) which successfully withstood a second vibration test.

9.2 Calibration and Alignment

The payload was designed to obviate the need for alignment of the various instruments with respect to each other. It was still necessary to align the individual collimator grids and to perform a number of calibrations of the collimator and the aspect camera.

Each collimator contained four wire grids. It was necessary that these grids be mounted so that the grid planes be parallel, and more important, that a plane could be found that contained one wire in each grid. (The grids were checked for uniformity before being incorporated into the collimators). A test facility for aligning the grids is shown in Figure 19. It consists of a point source of X-rays about 30 feet from the collimator.

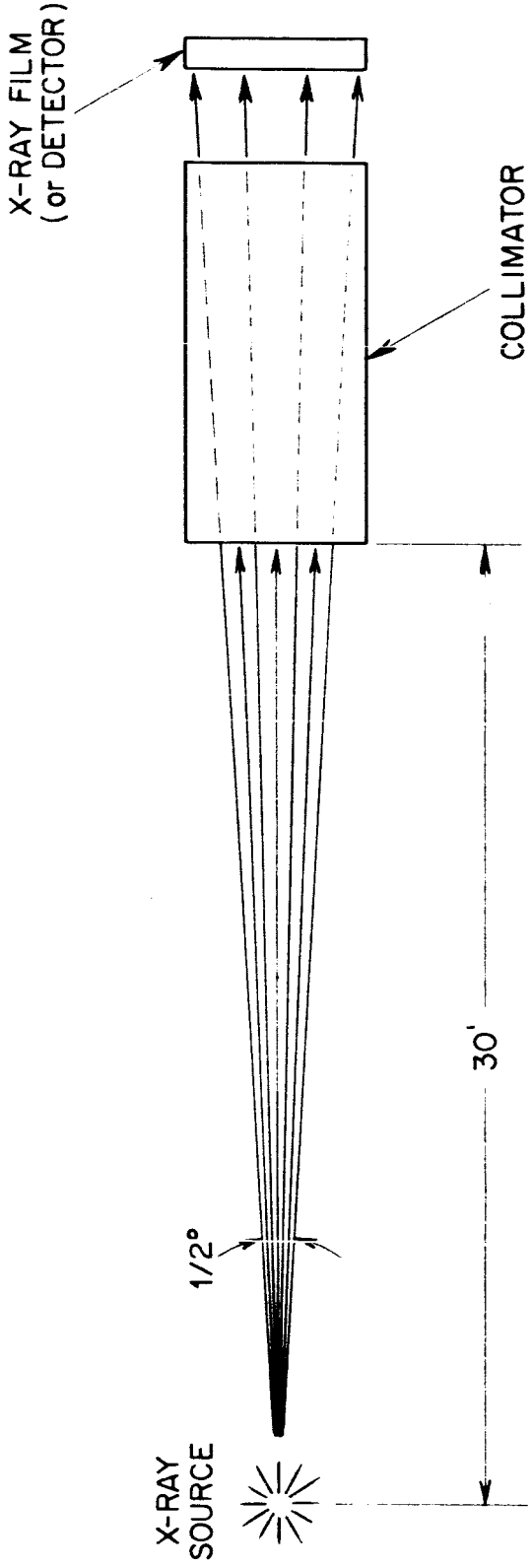

GEOMETRY OF COLLIMATOR TEST FACILITY

The X-rays were detected on film, we used a commercial X-ray cassette commonly used in medical radiography. With two or more grids in place, the X-rays were transmitted only along certain bands. The alignment was assured by requiring that the bands were parallel and uniform along their length as seen on the film. One example of an X-ray picture with all four grids in place is shown in Figure 20. The spacing between the bands as seen on the original photograph was about 0.5 inches which corresponds to an angular separation of 5' at 30 feet from the source.

With the aligned collimator a number of tests were performed; the most crucial of these was the so-called "fundamental experiment" in which we attempted to "locate" an X-ray source in the laboratory using the collimator and the aspect camera. The geometry of the experiment is shown in Figure 21. It is basically the same as the set-up shown in Figure 19 except that a visible light source was added that was copunctual with the X-ray source (hence our X-ray "star") and a slit placed in front of the collimator line. The collimator was rotated until a maximum was recorded in the X-ray counter behind the collimator. At that point, a visible light photograph was taken of the light source and the fiducial lights. One such photograph is shown in Figure 22. The X-ray "star" aligns with one of the fiducial band with a precision of about 5% of the band separation. The experiment was repeated over a wide range of transmission directions.

PHOTOGRAPH OF COLLIMATED X-RAY SOURCE

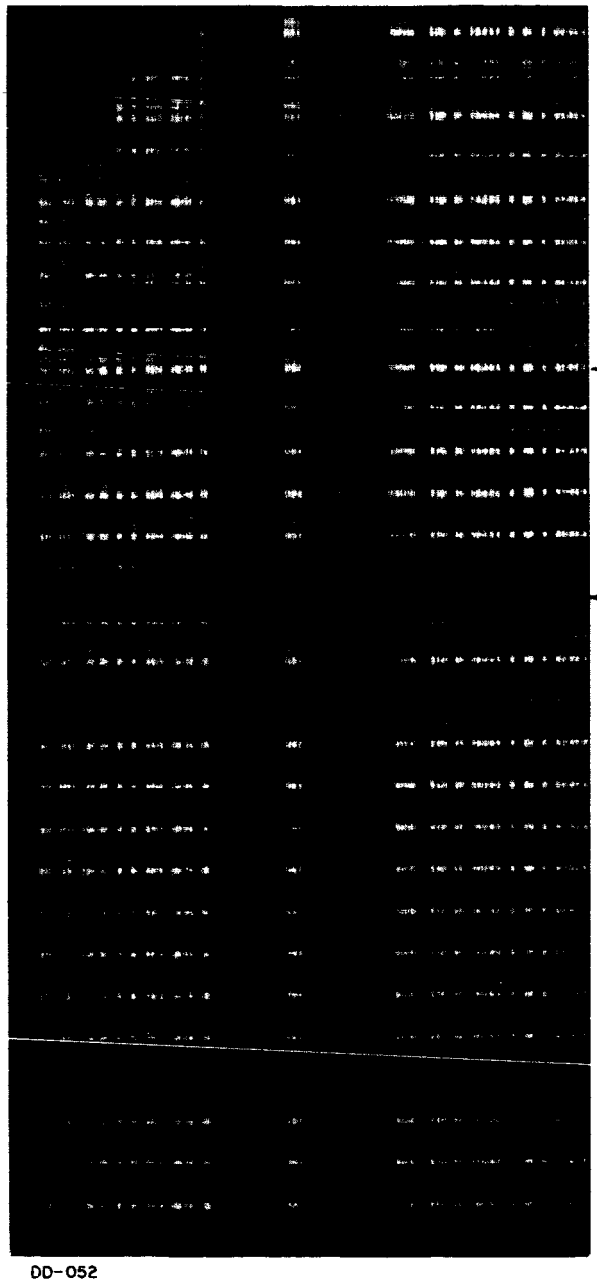

Figure 20

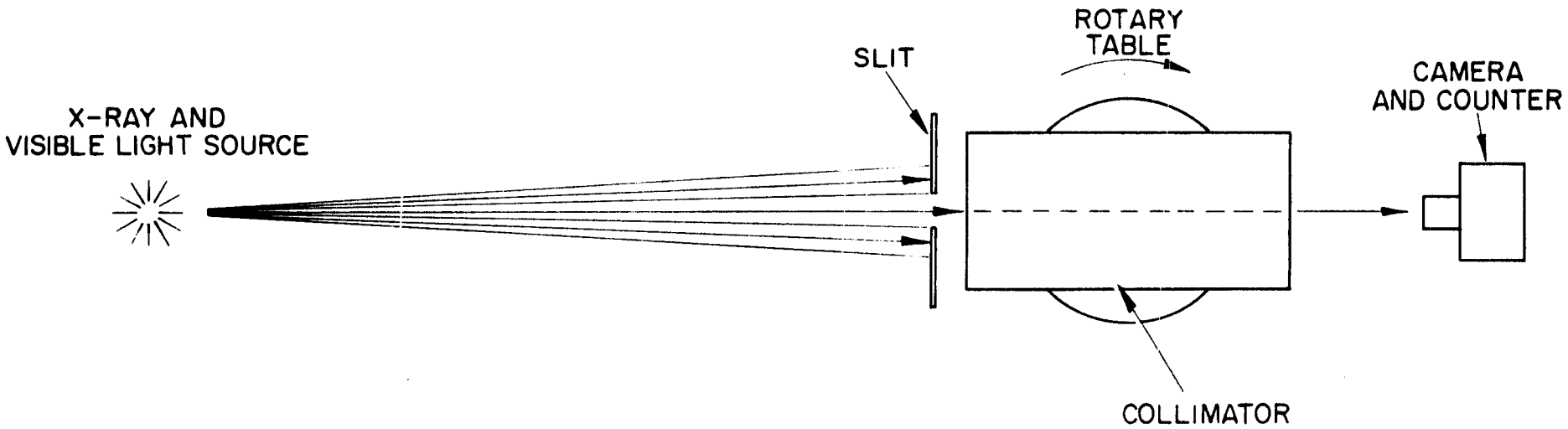

LAYOUT OF FUNDAMENTAL EXPERIMENT

Figure 21

ASPECT PHOTOGRAPH OF ARTIFICIAL X-RAY STAR

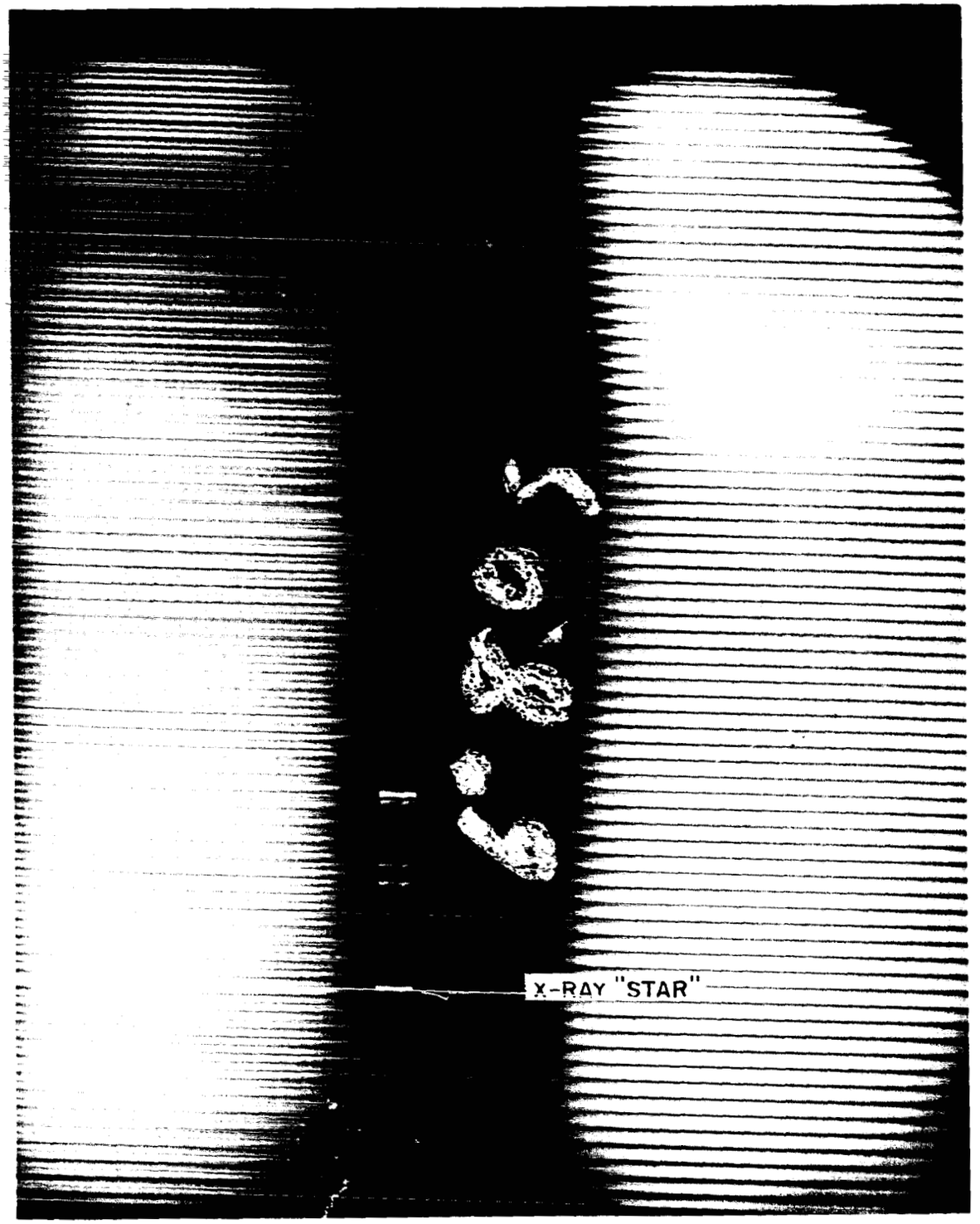

Figure 22

10.0 FLIGHT 4.148

Following final alignment and testing at AS&E, the payload was shipped to WSMR on 20 February, 1966.

The flight scheduled for 3 March was cancelled because of bad weather. The payload was operational at the time of the cancellation.

During the week preceding the launch attempt, we participated in a number of tests with the payload. We had no problems of any consequence with the instrumentation.

The flight was rescheduled for 8 March, the first opportunity to fly as allowed by the range. The payload plus rocket went through a vertical test and a five hour check without incident. The launch took place at 0 hr., 42 min. on Tuesday morning. The flight was successful. The rocket reached an altitude of 103 statute miles. All AS&E instrumentation functioned correctly. The ACS system apparently worked correctly and gave us not only the proper pointing but also the correct jitter rate during the hold period.

All data was recovered. The appearance of ScoX-1 was obvious in the data, even in real time. The payload was recovered with only minor damage.

11.0 PRELIMINARY DATA ANALYSIS

Preliminary analysis of the recovered data indicates that it will be possible to perform all experimental objectives. The data obtained during the time ScoX-1 was in view is shown in Figure 23. A series of peaks appear in the data, each one coinciding with a transit of the X-ray source across one of the transmission bands of a collimator. Between about T = 300 sec and t = 317 seconds, the rocket was virtually motionless and no source transits were observed. At about 325 seconds the rocket began its programmed roll (ledex position 21); at about same time aerodynamic forces began to take over to force the rocket nose down. Both of these effects cause the rate of motion of the source with respect to the collimator to increase markedly and resulted on a high rate of source transits until the source was lost entirely at about 335 seconds.

One of the aspect photographs taken during the flight is shown in Figure 24. We determined that the rocket followed its prescribed maneuver with about the expected precision; the Crab was acquired within about 1^{o} of the central axis of the collimators; and ScoX-1 within about 3^{o} of the central axis.

We expect the following results to arise from the analysis of these data:

1. Angular size and location of ScoX-1
2. Angular size and location of the X-ray source in the Crab Nebula
3. Energy spectrum of the X-rays from ScoX-1
4. Energy spectrum of the X-rays from the Crab Nebula

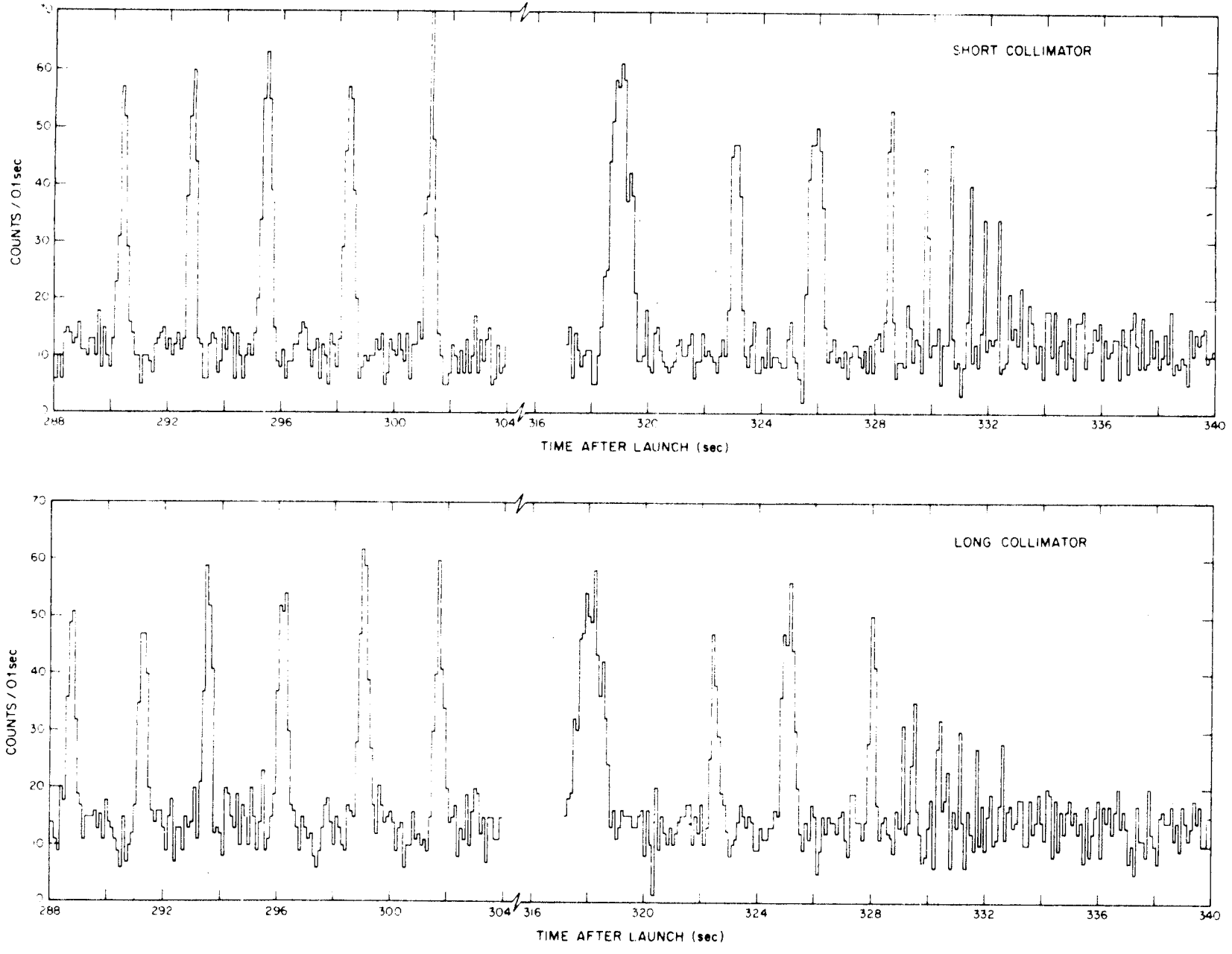

Figure 23

COUNTER DATA DURING Sco X-1 OBSERVATION

ASPECT PHOTOGRAPH DURING ScoX-1 OBSERVATION

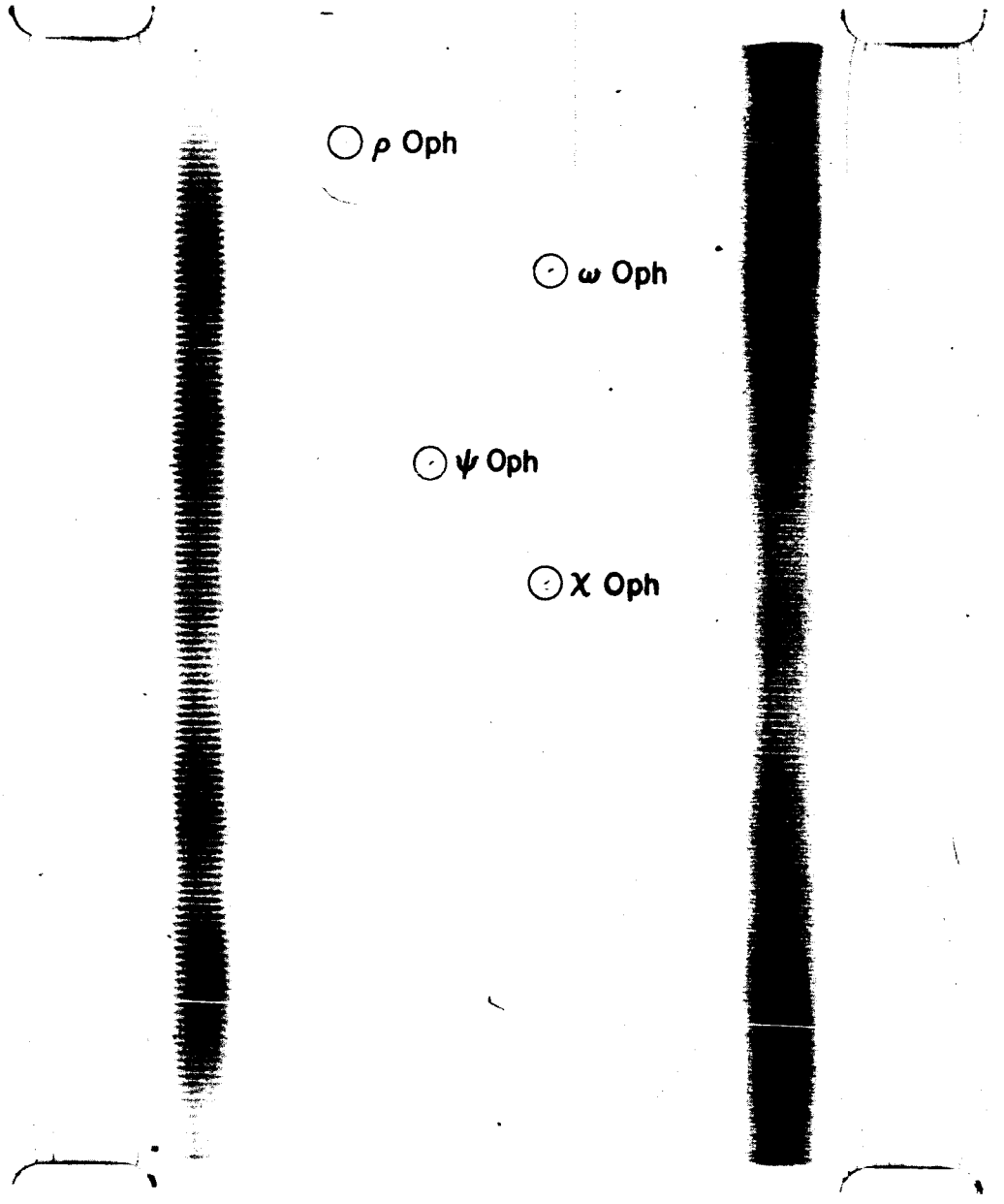

Figure 24

Because of its much higher X-ray flux, the data on ScoX-1 will be of higher precision than that obtained from the Crab Nebula.

APPENDIX I

Line of Sight Total Mass Computation

Introduction

A technique was developed to provide the total atmospheric mass along a line of sight in any arbitrary direction that passes within a specified altitude from the earth's limb. A computer program was developed to handle the computations as is applicable to any rocket or satellite vehicle, whether in or above the appreciable atmosphere regime. The analysis utilizes a model for the upper atmosphere that incorporates the effects of the dirunal bulge due to the solar heating. Other atmospheric models or tables could be introduced as needed to account for the variations due to sunspot activity over the 10 - 11 year cycle. In the present program, this is accounted for by minor changes in program constants, since it is a slowly varying function. Vehicle position and line of sight direction are used as integration constants for a routine that numerically integrates the air density per unit volume along the line of sight.

Results for an Aerobee Vehicle

The line of sight atmospheric mass per unit area was determined for the case of a typical Aerobee rocket launched from White Sands and reaching an altitude of 221 km. The local sidereal time at launch was $13^h\ 13^m$.

Air Mass in Micrograms/cm^2

Time (Sec)	h (km)	TARGETS*					
		Crab	ScoX-2	SgrX-1	Serp XR-1	Cyg XR-1	Cyg XR-2
80	107	3348	143	99	69	53	695
100	125	1801	82	57	40	31	371
120	146	882	46	32	23	18	188
150	175	349	21	15	11	8	77
180	198	173	13	9	7	5	41
230	220	96	8	6	4	3	24
250	221	97	8	5	4	3	23
280	217	107	14	6	4	3	25
330	192	233	65	10	7	5	40
390	132	1740	143	44	30	23	209

*The elevation angle of the Crab Nebula was below the local horizon and that of Cygnus XR-2 less than five degrees above the horizon at lift off. The other targets were at greater elevations ranging from ten to forty degrees.

APPENDIX II

1. INTRODUCTION

The discovery of significant fluxes of X-rays from celestial sources was made by Giacconi, Gursky, Paolini and Rossi (Giacconi, 1962), and subsequent rocket experiments by several groups have revealed as many as a dozen distinct X-ray sources (H. Bowyer, 1965). Most of these sources are clustered along the Galactic equator and within about 20° of the Galactic center. The most intense observed source, ScoX-1, in the constellation Scorpio at a Galactic latitude of 25° is the furthest removed from the Galactic equator. Up to now observations have been made primarily with gas counters operated in either the geiger or proportional region with a field of view limited by mechanical collimators. The angular resolution has been typically degrees of arc. However, it is possible to build collimators for X-rays of very high resolution since diffraction effects are negligible. For any finite size opening, one is limited only by the precision of fabrication. The modulation collimator devised by Oda (Oda 1964) and first used by Oda et al (1965) in a rocket experiment represents a means of achieving high angular resolution with a relatively simple device. We have made further use of modulation collimators to devise a rocket payload exclusively devoted to making high resolution observations of single X-ray sources in order to determine the angular size and location of these objects. The payload was successfully flown on an Aerobee rocket on 8 March 1966 from the WSMR. Analysis of the data from that flight has demonstrated that the angular size of ScoX-1 is less than 20 arc seconds (Gursky 1966A), and has yielded a location that is precise to about 1 arc minute. (Gursky, 1966B). On the basis of the location, a tentative identification has been made of the visual counterpart of the X-ray source (Sandage, 1966).

Except for the fact that we have built a larger and higher angular resolution modulation collimator than hitherto, the uniqueness of the present experiment lies in certain innovations in the collimator and in the optical aspect system that have enabled us to measure location with high precision. Grazing incidence telescopes with better than 1 arc minute resolution are being constructed for solar X-ray studies, however, because of limitations imposed by currently available sounding rockets, the instrument configuration utilized in this payload offers the most immediate means for obtaining high angular resolution data in X-ray astronomy.

II. NEED FOR HIGH ANGULAR RESOLUTION DATA

One known object, the Crab Nebula, has been positively identified as one of the X-ray sources. (Bowyer 1964). There is tentative evidence for X-ray emission from Cas A, Cygnus A, and M-87 (Byram 1966) however, the majority of the X-ray sources do not correlate with obvious celestial features. The necessity for making positive identifications of the X-ray source is clearly important. Observations in X-ray astronomy are limited by the availability of space platforms (only 15-20 min/year of observation time has been utilized so far) and the general difficulty of performing space experiments. Thus provided that good position data is available, it is likely that major advances in our understanding of the X-ray sources will come from observations in the visible light and the radio portions of the electromagnetic spectrum.

Theoretical indications are that reasonably bright visible and radio counterparts should exist for the X-ray sources. The observed flux density in X-rays is typically 10^{-25} to 10^{-26} ergs/cm^2 -sec-(c/s); if the physical mechanism for the production of the X-rays is either electron bremsstrahlung in a hot plasma or the synchrotron radiation of high energy electrons (c. f. Manley, 1966) the flux density at longer wavelength should equal or exceed this figure. The integrated power in visible light must then be at least 10^{-10} to 10^{-11} ergs/cm^2 -sec which would correspond to an object

of 12-14 magnitude, barring obscuration. Provided the angular size of the emission region does not exceed the point where the surface brightness is below the limits of detectability (1-2 arc minutes), the object should be clearly visible.

If the X-ray source is a neutron star, the X-ray spectra would be that of a black-body and the visible light emission would be several orders of magnitude smaller. However, theoretical arguments have been presented that indicate that the cooling time for neutron stars is too short to make them likely candidates for the X-ray sources, and experimental data indicates that the high energy end of the X-ray spectrum from at least several of the sources is not of a black-body form.

Unless a finite angular size can be measured for an X-ray source, the possibility must be considered that the visible counterpart is a star-like object with little or no measurable size. There are about 8×10^6 14 mag. or brighter stars in the sky, corresponding to an average density of about $200/deg^2$. Within a ten degree band around the galactic equator the density rises to over $400/deg^2$. Since most of the X-ray sources are close to the galactic equator, location measurements precise to arc minutes must be obtained in order to find the visual counterparts with reasonable certainty. If the X-ray source can be shown to have finite size, the identification problem is eased considerably because of the much smaller density of such objects in the sky of the required brightness. Angular size is of intrinsic importance since it must be known in order to determine the energy density in the source. It was these considerations that led us to the conclusion that high angular resolution observations of the X-ray sources were possibly the most important that could be performed at the present time.

III. General Design Considerations

The problem of designing the instruments to perform this experiment can be stated in terms of the following requirements.

1. High angular resolution (1 arc minute) X-ray collimator

2. Adequate detector area. For ScoX-1 we measure a counting rate of about 20 counts/cm^2 - sec in thin window gas counters, thus observation with a 100 cm^2 effective area counters for several seconds is more than sufficient. For the weaker sources whose X-ray flux is 1/10 to 1/20 of ScoX-1, correspondingly longer observational time is required.

3. Precise aspect system. It must be possible to continuously relate the X-ray collimator axis to the celestial sphere. This can only be done conveniently with high precision by observing the star field. A corollary to this requirement is the necessity for alignment of the aspect system with the X-ray collimator.

The rocket carrier represents an intimate part of the experiment. We had available the Aerobee 350 equipped with a roll - stabilized, attitude control system (ACS), with which the entire payload could be aligned to a programmed direction. The stabilization made use of gas jets that kept each of the three rocket axes within prescribed limit cycles around their respective programmed orientation. The attitude reference was a set of gyros, and the attainable pointing precision with this system was about 2^o. Residual motion within the limit cycle could be reduced to several arc minutes/second and the size of the limit cycle could be made a fraction of a degree. The rocket could be manuevered to as many as five separate targets during a single flight. Total observation time above the atmosphere is about 250 sec, but actual time on target may be substantially less depending on the manuevers. Clearly this system, particularly the pointing precision, sets well defined limitations on what observations can be performed during a flight.

The modulation collimator, since it can be built with large open area for X-rays and has a broad field of view for detecting a source, is well suited for use in an experiment with the ACS controlled Aerobee. The principle of operation of the collimator is shown in Fig. 1. In its simplest form, the collimator consists of two planes of parallel wires or grids. For parallel radiation, the front wires cast a sharp shadow on the plane of the rear wires.

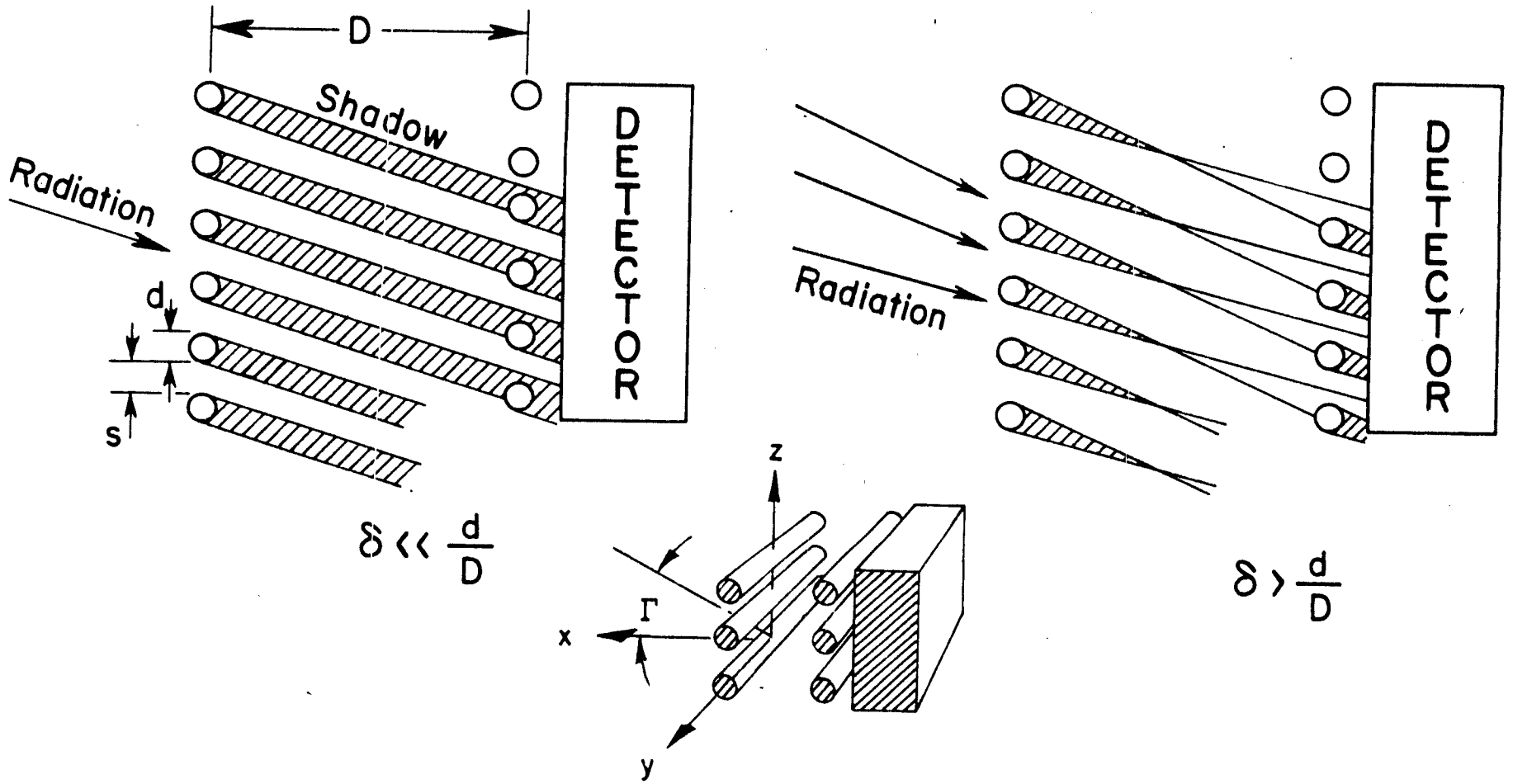

Figure 1

PRINCIPLE OF MODULATION COLLIMATOR

If the shadow falls on the open area between the wires, no transmission occurs; if it falls on the wires themselves, the collimator transmits radiation. High angular resolution is achieved only in the plane normal to the wires. As the angle of incidence of the radiation (as measured in a plane that is normal to the direction of the wires) varies, as during a scan across an X-ray source, the collimator alternately transmits or obscures (modulates) the radiation. If the incident radiation is not parallel (as would be the case for a finite diameter source), the shadowing is not complete and the modulation will not be complete. The angular response of this form of the modulation collimator is shown in Figure 2. The resolution is determined by the quantity $\delta = (s + d)/D$, which is the width, at the base of the modulation cycle. Modulation will disappear for an X-ray source whose angular size is larger than δ. The addition of intermediate grids at the proper spacing will obscure certain directions and extend the range of angular sizes that can be observed. An example is Figure 3. The angular resolution is still given by δ, but the transmission directions of the collimator are separated by an angle 4δ. With the additional grids the modulation collimator is essentially a one-dimensional image dissector.

We have currently been building modulation collimator grids by using standard photo-etching and electroforming techniques, as well as by winding wire around a specially machined form. Figure 4 is a photograph of 4 x 8" wire wound grid that has 0.005" diameter wires on 0.01" centers. The effective area of this particular grid is about 40 percent. In principle only 50 percent open area can be achieved; however, necessary structural elements will reduce the open area even further.

A single transit across a source with a conventional collimator yields the location of the source along a single line on the celestial sphere. However, with a modulation collimator since its angular properties are only weakly dependent on the angle of incidence, the source location may be along any of a series of parallel lines, each one corresponding to a peak

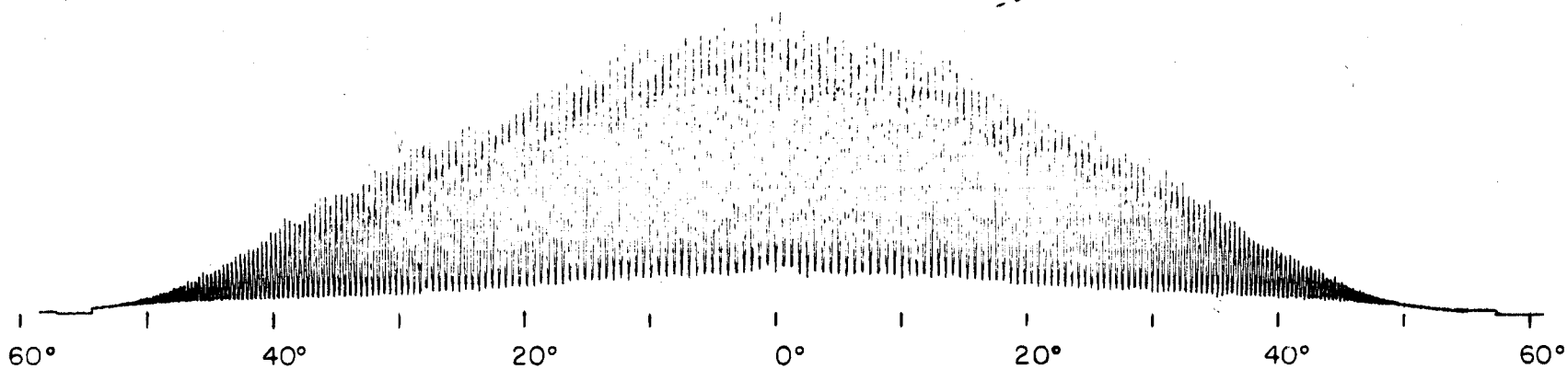

AA-234

Figure 2

ANGULAR RESPONSE OF MODULATION COLLIMATOR
(VISIBLE LIGHT)

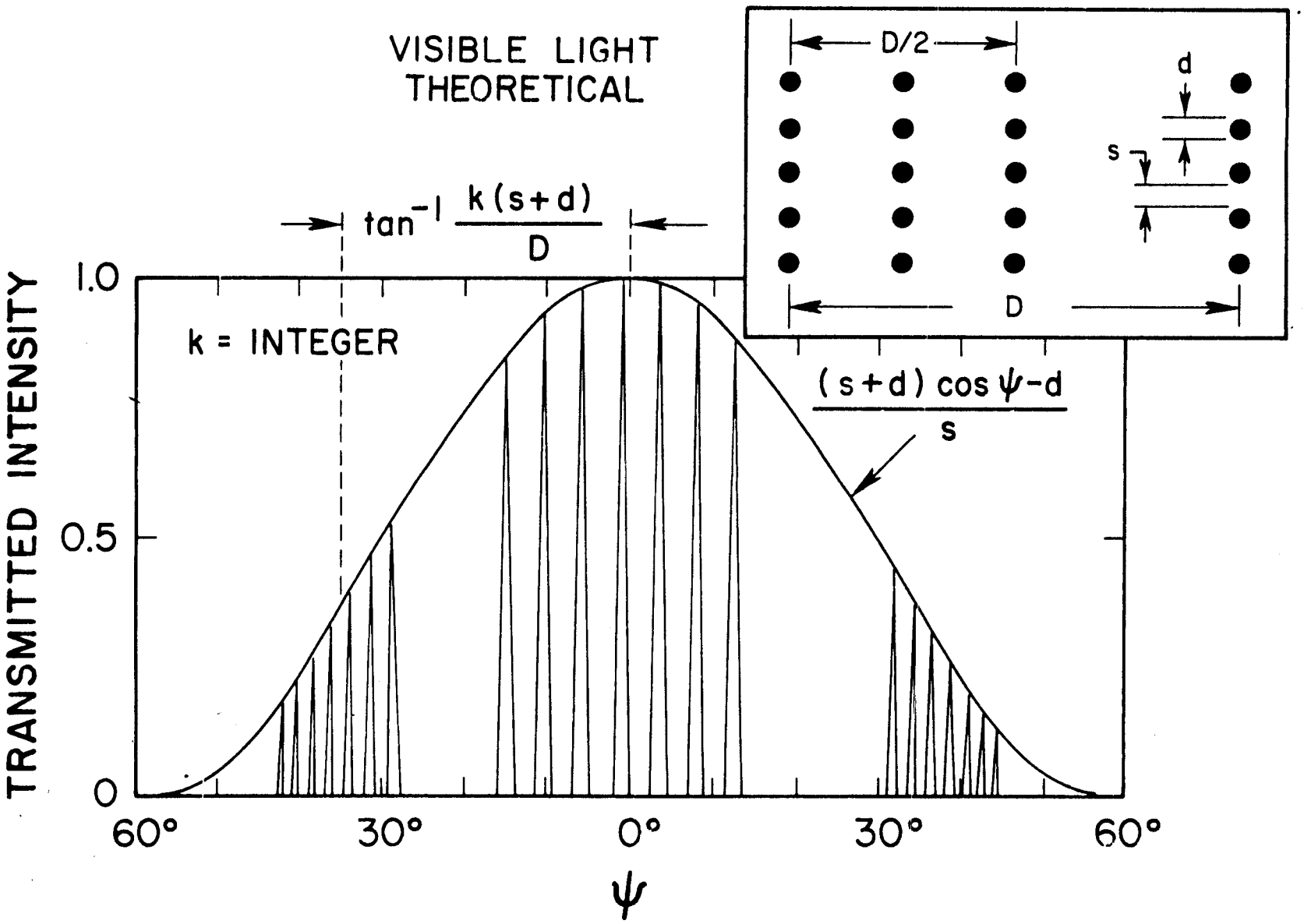

ANGULAR RESPONSE OF MODULATION COLLIMATOR AS MODIFIED BY ADDITIONAL GRIDS

Figure 3

WIRE GRID COLLIMATOR

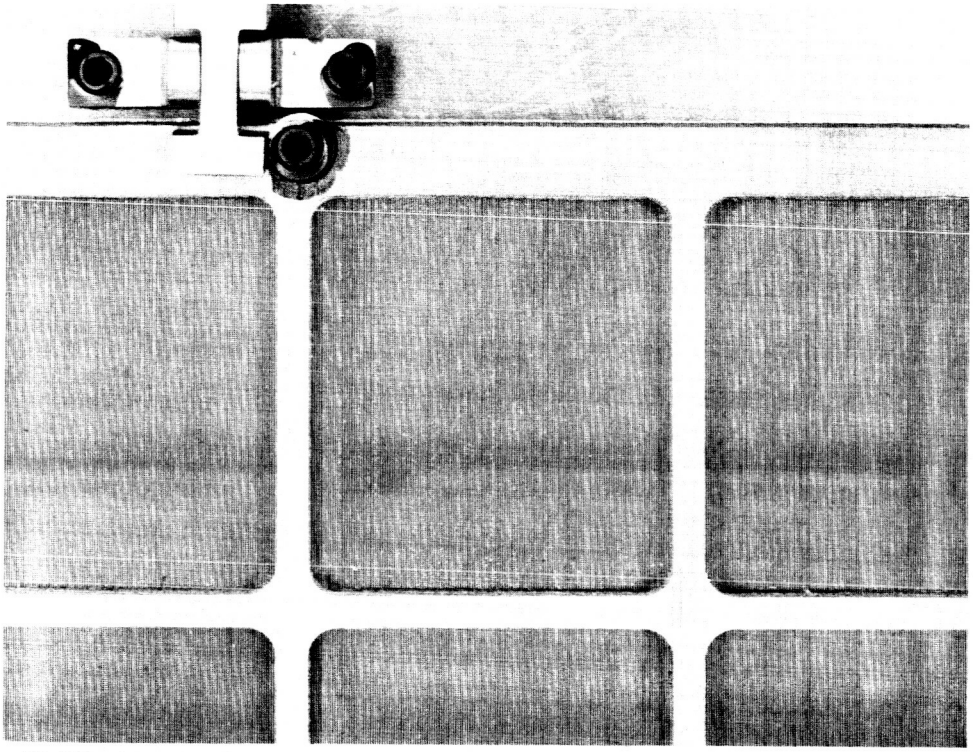

DO-005

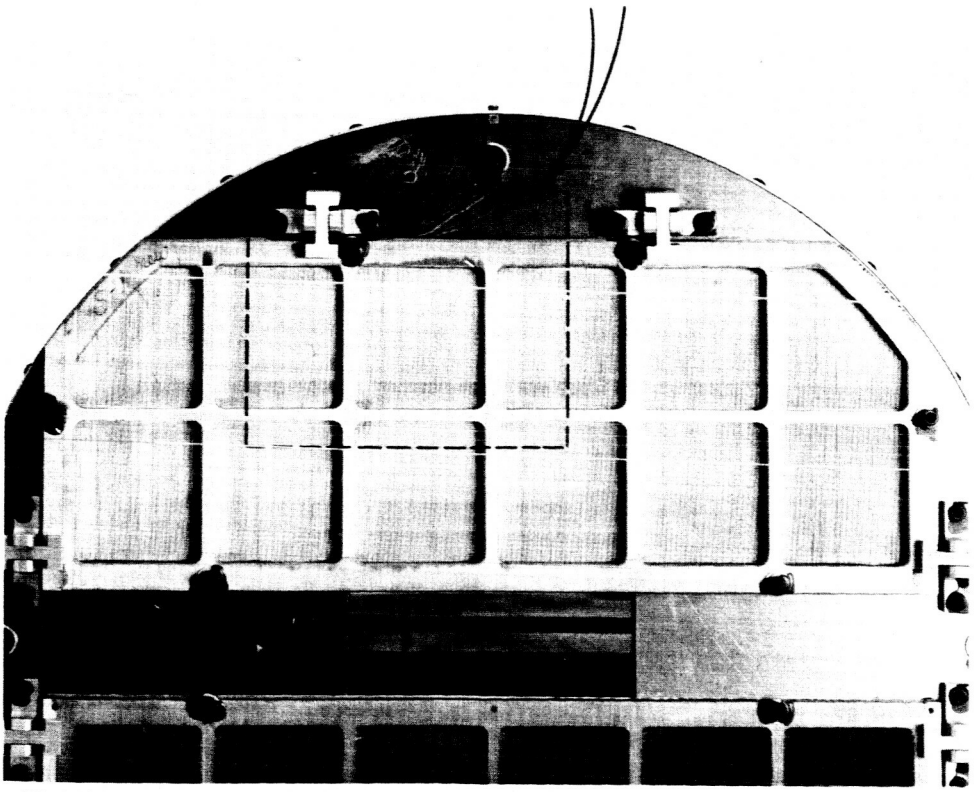

DO-004

Figure 4

in the angular response of the collimator (see Figure 3). However by making independent observations of the X-ray source through two slightly different modulation collimators which have a common field of view and parallel X, Y axes, the number of possibilities can be reduced, by a kind of vernier effect, to one, or at most, a few lines. If the two modulation collimators are constructed such that there is a small difference in the separation, D, between the grids, a source transit in each will define a set of lines in the sky with slightly different spacings. Since the lines in the two sets will be parallel to each other, the source there will be a single line (or lines) that is common to the two sets, and clearly the source must be on the line. In order to determine where along the line the source is located, the observation must be repeated along a different scan direction by rotating around the Z axis. This will yield another line along which the source must lie, but tilted with respect to the first, and the source must be at the intersection of the two. There are several alternate schemes by which one or more modulation collimators can be used to provide a unique source location.

The utilization of a high resolution X-ray detection system allows the measurement of physical size or structure of an X-ray source but does not, by itself solve the problem of locating the source on the celestial sphere. An actual experiment consists simply of recording the counting rate from the X-ray detectors as a function of time from a platform in space whose orientation or motion is not known with any precision. The corresponding experiment if performed from the surface of the Earth would yield location almost directly since both the orientation of one's measuring instruments with respect to the Earth and the celestial orientation of any axis on the Earth can be determined with almost arbitrary precision. In a space-borne experiment it is necessary to obtain a continuous record of the celestial orientation. Since this involves a separate set of instruments it immediately brings up the problem of measuring the relative orientation of two sets of instruments and maintaining that orientation throughout the rocket flight.

We have devised a means of measuring orientation that avoids both these problems. It involves photographing through the one lens of an aspect camera, both the star field and a set of fiducial lines are formed by allowing diffuse light to be incident on the collimator, which from a simple point of view will be transmitted preferentially along the allowed directions as defined by the angular response of the collimator. For each allowed direction a bundle of parallel rays is formed, which produces the image of a line by a lens focused to infinity.

The net result is a series of lines that map out the angular response of the collimator. The same lens is allowed to view the star field through an opening in the collimator. The image of each fiducial line defines a locus of directions in space from where X-rays may arrive; each star image defines a unique celestial orientation in space. This solves the orientation problem since measurements can be taken with high precision from the resulting photograph. There is no requirement to align the camera with respect to the modulation collimators, or to rigidly couple the camera to the modulation collimator.

Figure 5 shows the geometry of camera with respect to the modulation collimator, and Figure 6 is a photograph of the stars and fiducial lines recorded during flight. In actuality the fiducial lines present a very complex structure because the transmission of visible light through the collimator is dominated by diffraction and it is not obvious where the fiducial line image coincides with the peak of the X-ray transmission band. To answer the question precisely we did an experiment which consisted of measuring an artificial X-ray "star" with the collimator and the aspect camera. The

artificial star consisted of a point X-ray source colinear with a point light source. The X-ray source was observed through the modulation collimator which was rotated until a maximum transmission was observed. At that point an aspect photograph was taken. A series of measurements made this way confirmed with a precision of about 5% of the separation of the fiducial bands, that the X-ray direction as determined from the image of the visible counterpart of our artificial star coincided with the brightest portion of the fiducial line. We also noted that as one went off axis, the point of coincidence shifted systematically. In the analysis of flight data we restricted our measurements to fiducial lines near the central portion of the field of view.

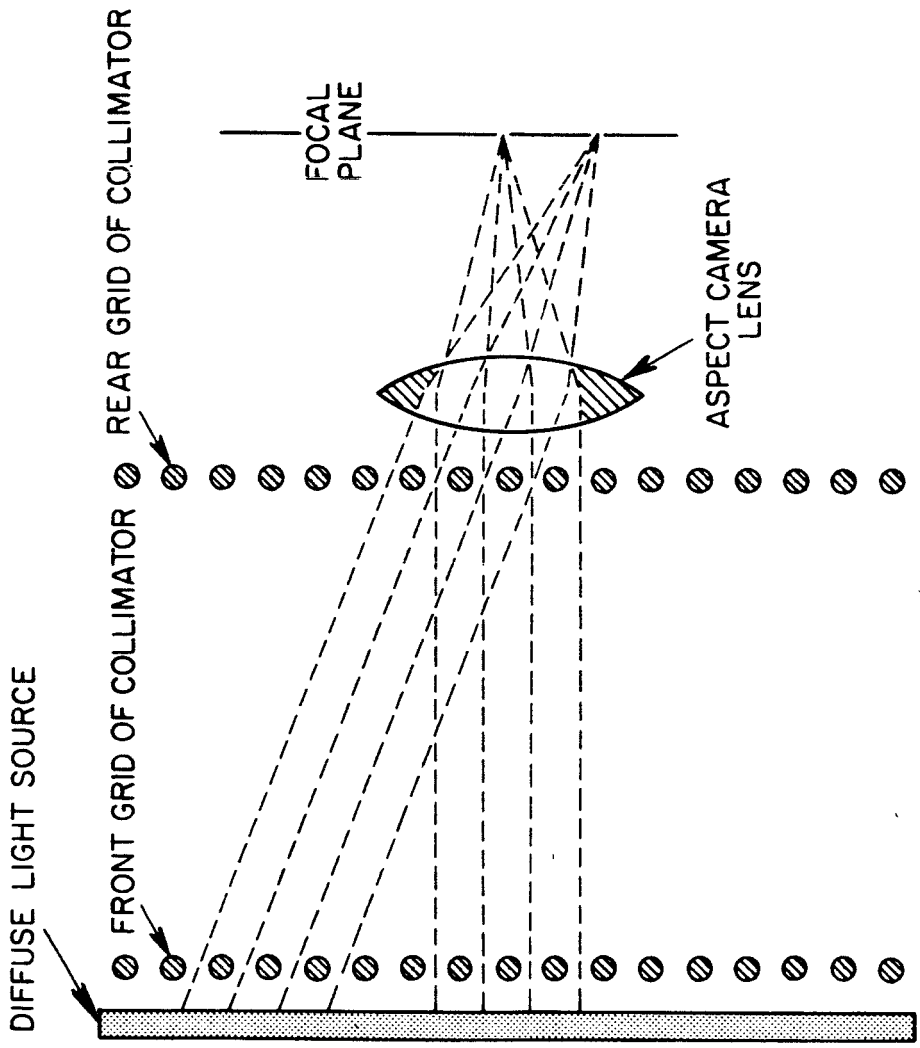

FIDUCIAL LIGHT GEOMETRY

Figure 5

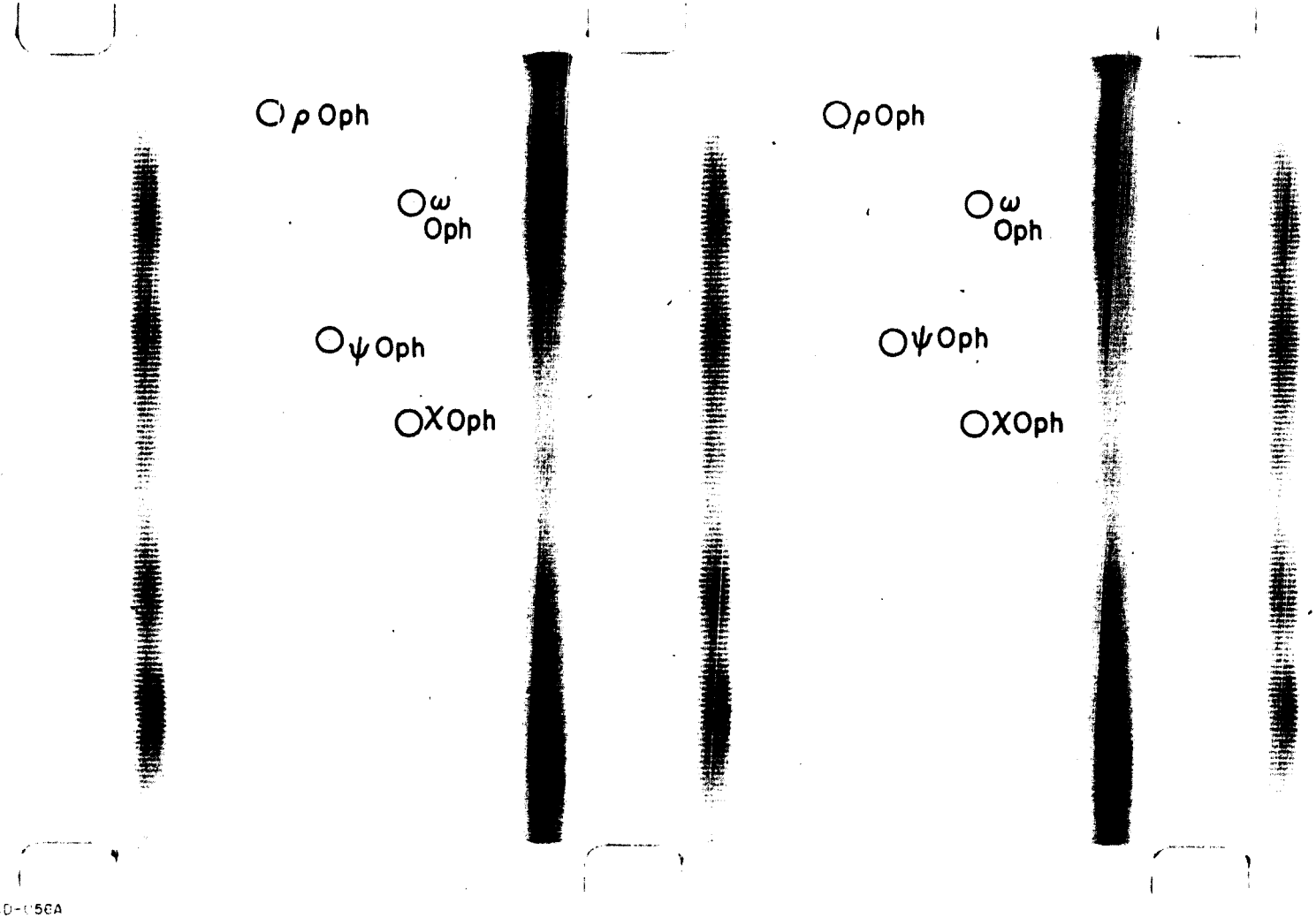

CD-C5CA

Figure 6

SUCCESSIVE PHOTOGRAPHS OF STAR FIELD AND FIDUCIAL MARKS TAKEN DURING ROCKET FLIGHT

IV. DESCRIPTION OF THE ROCKET PAYLOAD

The individual instruments that made up the payload were the modulation collimators, the X-ray detectors, the aspect camera and associated electronics. The specifications on the instruments are listed in Table I. The two modulation collimators used to achieve the vernier effect are mounted in a common cylindrical housing. The aspect camera is mounted below the modulation collimators and looks out through an opening between the collimators. The X-ray detectors are also mounted below the collimators. The several instruments are shown in Figure 7 and the assembled payload is shown schematically in Figure 8. An actual observation during a rocket flight consists of pointing to a known X-ray source with whatever precision is permitted by the rocket control system. As the rocket drifts back and forth within the limit cycle, the X-ray source will move across the transmission bands of the modulation collimators. Thus a scan is obtained over a very limited portion ($\sim 1/2^{\circ}$) of the celestial sphere. Figure 9 shows the X-ray detector data obtained during a rocket flight of 8 March 1966. The peaks in the data result from successive transits of ScoX-1, the strong X-ray source in Scorpio. These data plus others were analyzed to yield a location for the source and an upper limit to the angular size of the source. The Crab Nebula was observed during the same flight, both as a test of the instrumentation since its location is well known, and to obtain more information on that object as an X-ray emitter.

The capability of this instrumentation can be summarized as follows. The modulation collimators have an angular resolution (defined as the full width at half maximum of the individual transmission bands) of about 40 arc seconds. Given any reasonable signal/noise, the centroid of the counting rate peak observed when traversing a small diameter source will be a fraction of this (c.f. the data in 9). The separation between peaks is about 5 arc minutes, thus a source of several arc minutes size can be resolved into 40 arc second bands. With the present length (D) collimator, which

ASSEMBLED PAYLOAD

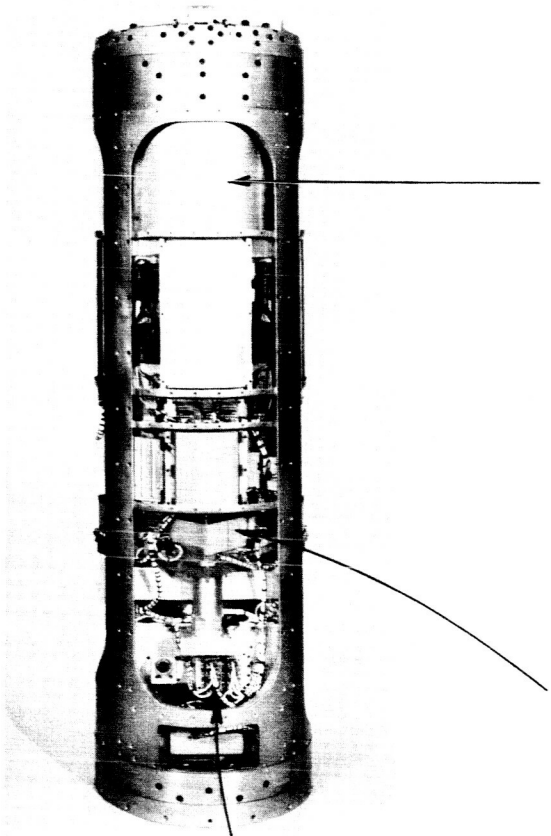

DD-044

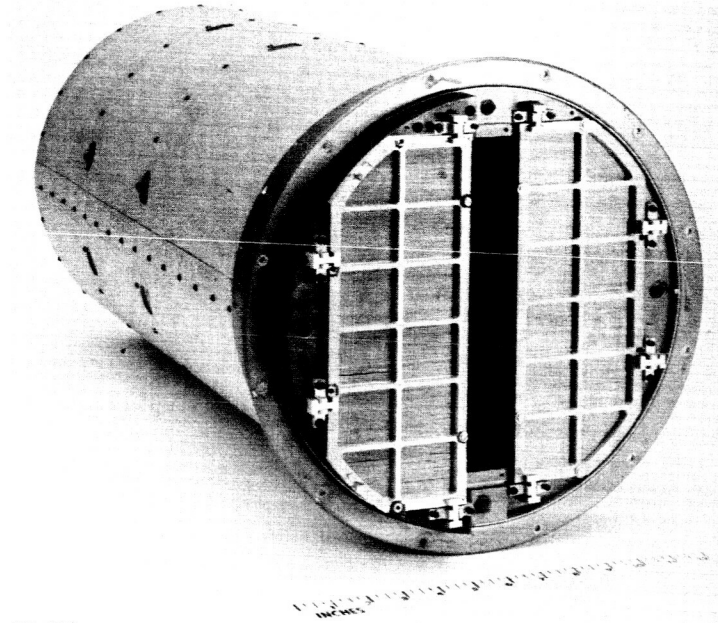

DD-003

MODULATION COLLIMATOR

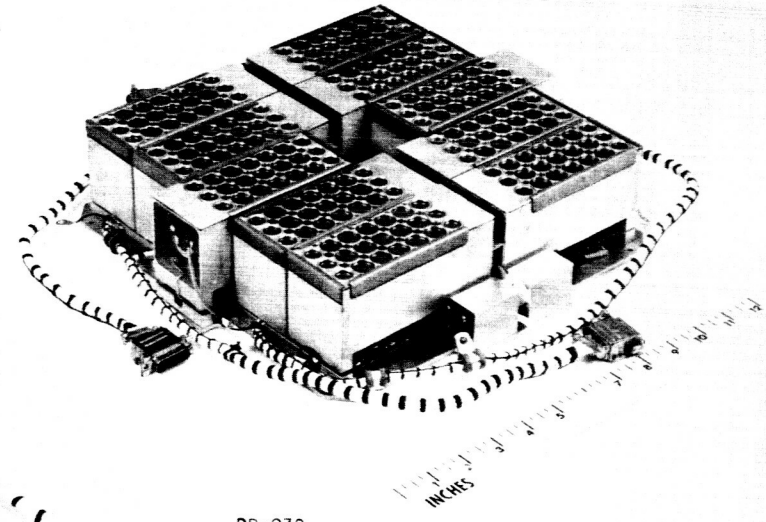

DD-038

PROPORTIONAL COUNTERS

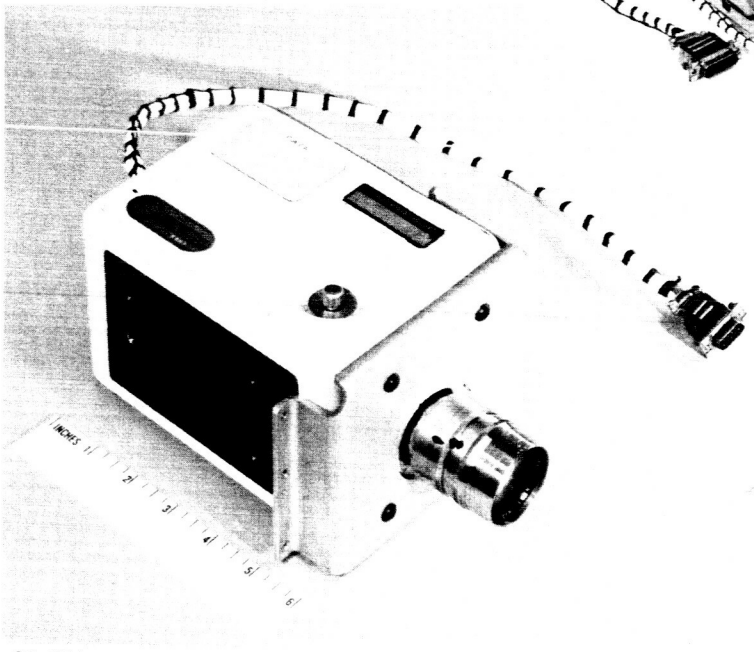

DD-034

ASPECT CAMERA

Figure 7

LAYOUT OF PAYLOAD INSTRUMENTATION

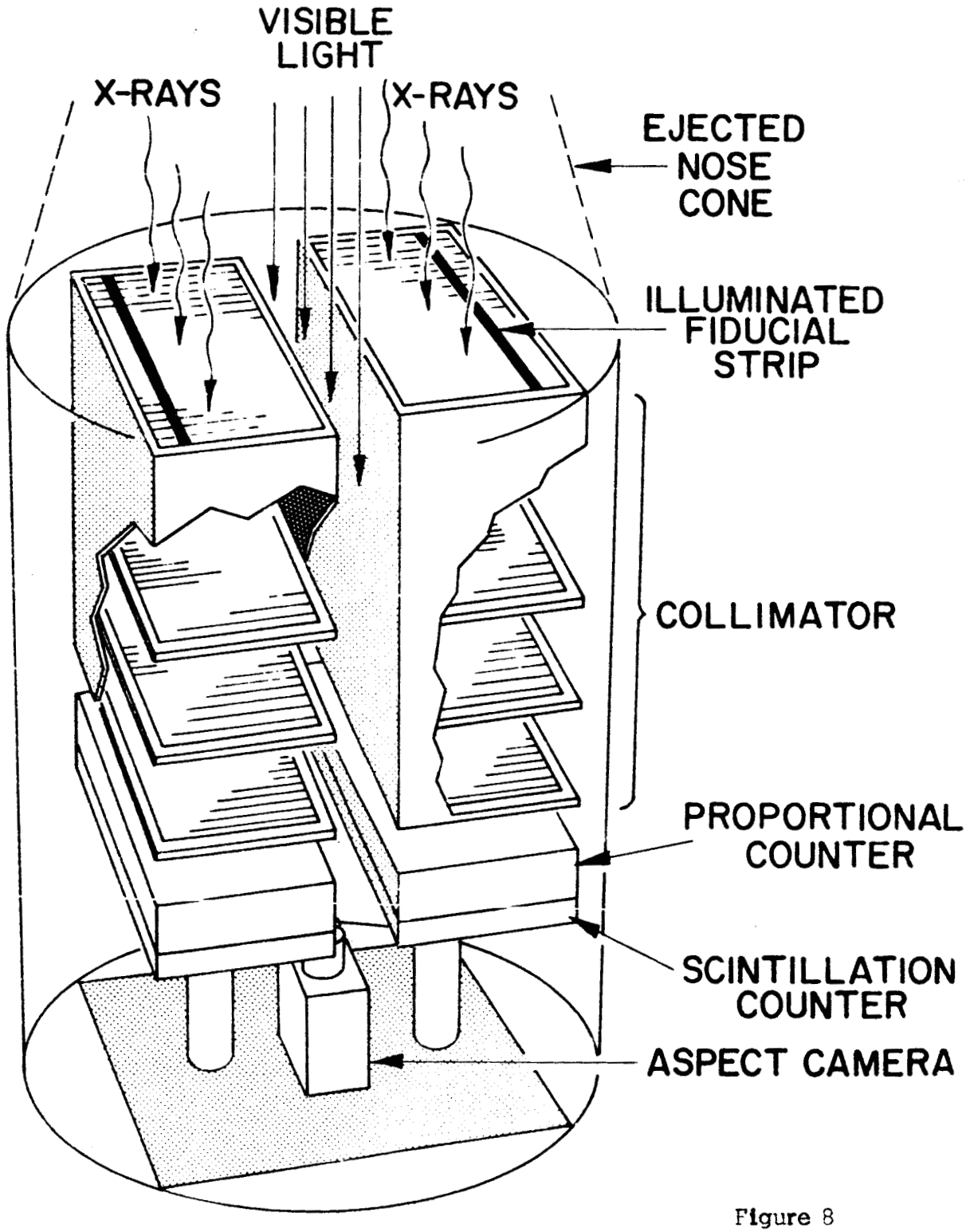

Figure 8

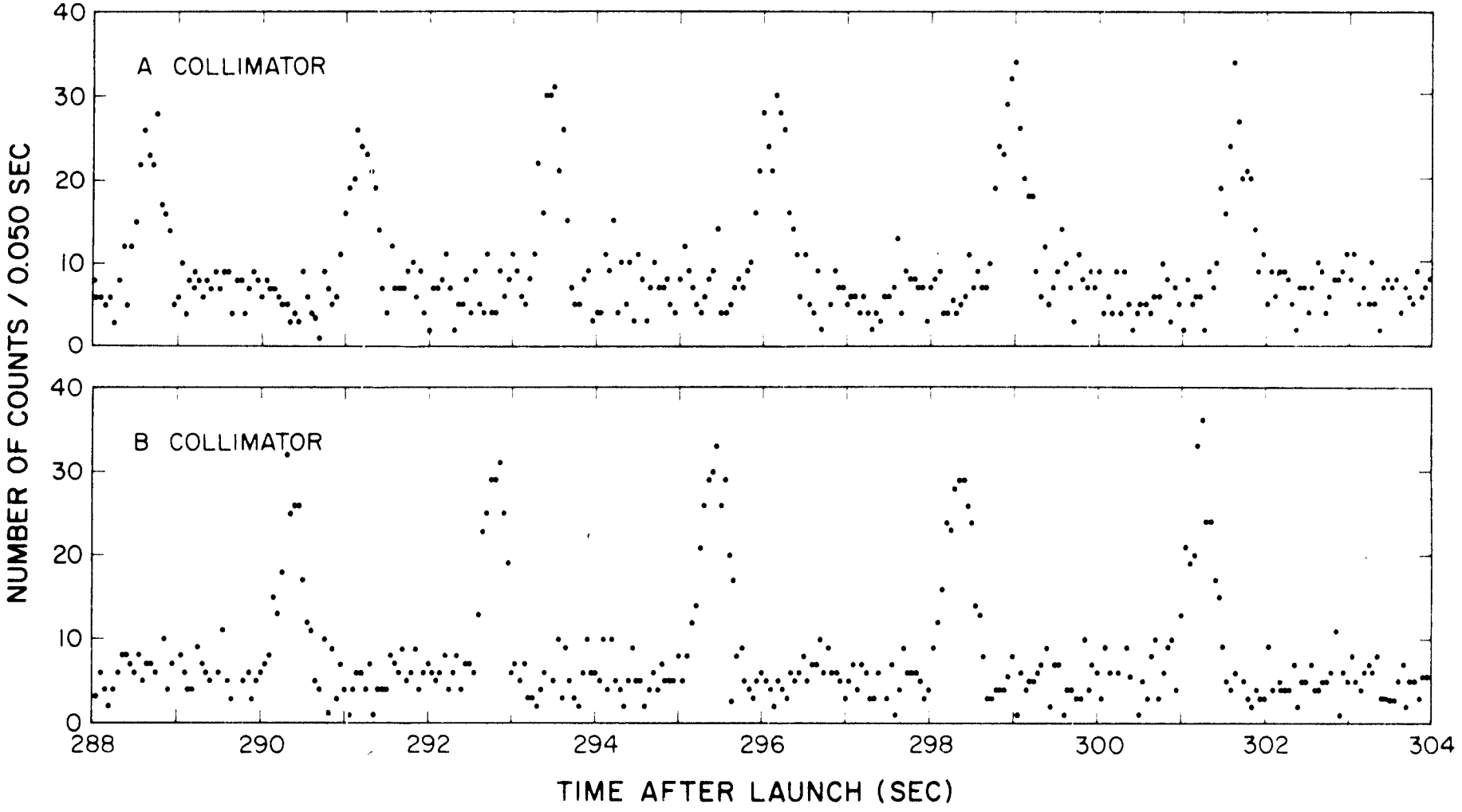

Figure 9

SUCCESSIVE TRANSITS OF SCOX-1 DURING FLIGHT

Table I: Instrument Specifications

Modulation Collimators

	Long Collimator	Short Collimator
s	0.0045"	0.0045"
d	0.0055"	0.0055"
D	25.125	25.000
	1463×10^{-3}	1.535×10^{-3}
# of intermediate grids	2	2
separation between adjacent transmission bands	-------	-------
Peak X-ray Transmission	40%	40%

Aspect Camera

Body	16 mm Millikan (Model DBM - 3c
Lens	f1:4 50 mm Cooke
Field of View	3×10^{o} for stars
Film	Tri-X on Estar Base

X-ray Detectors

Operating Mode	Proportional Region
Gas Filling	Xenon at one atmosphere
Entrance Window	9.0 mg/cm^2 Beryllium
Effective Area	125 cm^2 per collimator
	(made up of 5 individual counters)

is limited by the Aerobee rocket. the angular resolution can not be improved (by using finer grids) by more than a factor of 4 before X-ray diffraction effects start becoming important. The present aspect camera allows photographing 6-7 the magnitude stars provided the drift rate of the rocket does not exceed several arc minutes/second. The center of the star images on tri-X film can be located to within several microns which represents about 10 arc seconds with a 50 mm focal length lens. The celestial orientation of the X-ray collimators could be determined with comparable precision anywhere on the star photographs except at the corners where distortions were not negligible.

With this instrumentation used on Aerobee rockets it will be possible to make observations on all but perhaps the weakest of the presently known celestial X-ray sources. Given longer observation times as would be available from an orbiting vehicle, observation time and sensitivity could be extended. However as the sensitivity is improved. the density of observable sources will no doubt increase and a means of limiting the field of view must be provided in order to reduce the problem of confusion between adjacent sources.

The rocket payload described here was developed under NASA contract NAS W-1284. Our colleagues have greatly contributed to the program. They are Dr. R. Giacconi. Dr. P. Gorenstein, Dr. J. Waters at AS&E and Professor H. Bradt. Professor G. Garmire and Dr. B. V. Sreekantan at MIT.

REFERENCES

Bowyer, S., Byram, E. T., Chubb, T. A. and Friedman, H.

_____ 1964, Science, 146, 912;

_____ 1965, Science, 147, 394

Byram, E. T., Chubb, T. A., and Friedman, H.; Preprint, 1966

Giacconi, R., Gursky, H., Paolini, F. and Rossi, B.

_____ 1962, Phys. Rev. Letters 9, 439

Gursky, H., Giacconi, R., Gorenstein, P., Waters, J. R., Oda, M., Bradt, H., Garmire, G., Sreekantan, B. V.;

_____ 1966a, Ap. J. 144, 1252;

_____ 1966a, Ap. J. - to be published

Sandage, A. R., Osmer, P., Giacconi, R., Gorenstein, P., Gursky, H., Waters, J. R., Bradt, H., Garmire, G., Sreekantan, B. V., Oda, M., Osawa, K., Jugaku, J.

_____ 1966, Ap. J. - to be published

Manley, O.; 1966, Ap. J. 144, 1253

Oda, M.; 1965, Applied Optics, 4, 143

APPENDIX III

System Testing

The systems tests performed on the payloads included electrical tests, static load tests, vibration tests, vacuum tests, and payload telemetry integration tests.

Static Load Tests

Static load tests were conducted in accordance with the loads shown in Figures 1 and 2. Deflection as measured at the nose cone tip was, for both payloads less than the 0.364 in. maximum allowable specified by NASA. Also, for both payloads, the permanent set measured after removal of load was less than 10 percent of the deflection.

Electrical System Tests

Electrical system checks were conducted on the completely assembled payload which established: (a) proper operation of the instrumentation, power and control systems, (b) door and tip ejection systems, (c) correct data readout at the telemetry interface and (d) compatability with the ground support test console. Satisfactory completion of this test was aprequisite to committing the payload to vibration tests.

Vibration Tests

Both payloads successfully passed random noise vibration tests at the following test levels.

Payload Axis	Level	Duration
Longitudinal	10 GRMS	1 minute
Each transverse	6.2 GRMS	1 minute

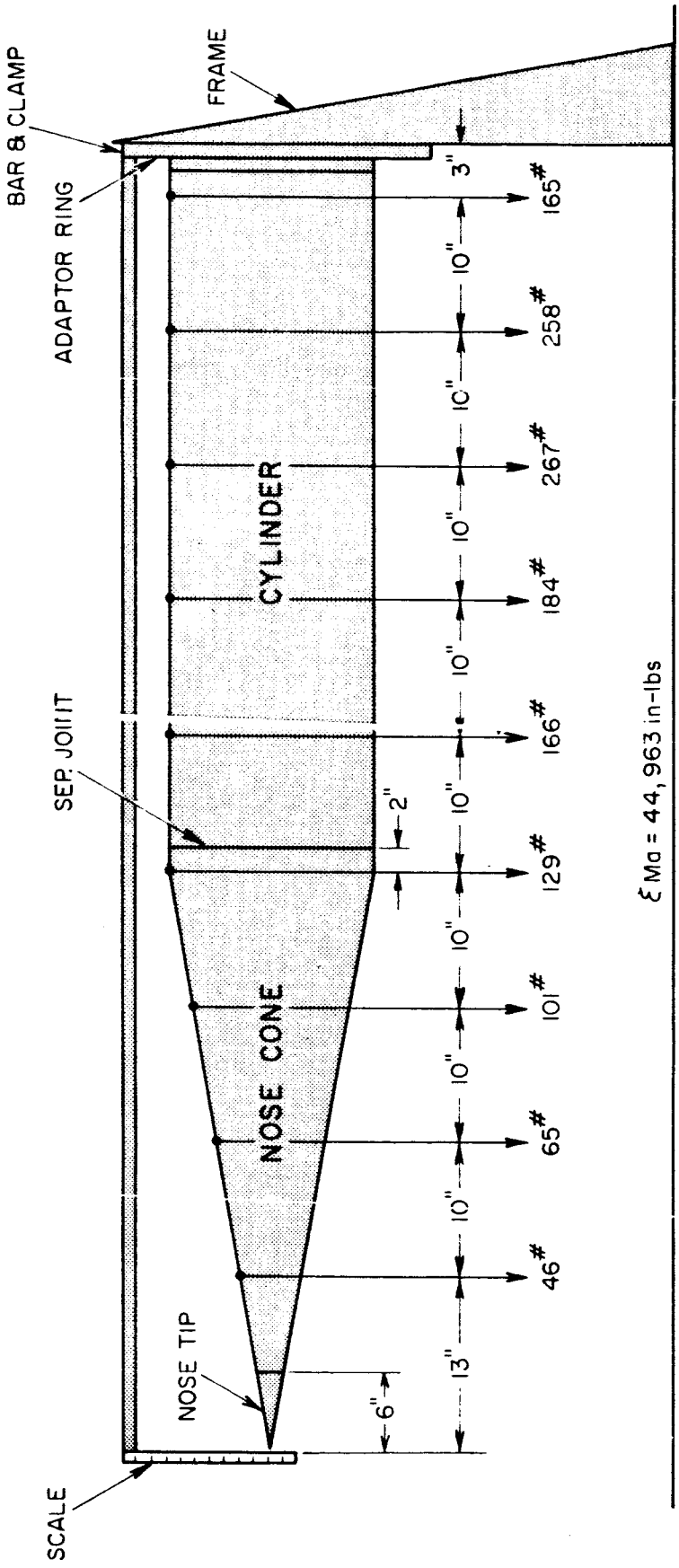

4.148 CG NASA ROCKET BENDING MOMENT TEST

Figure 1

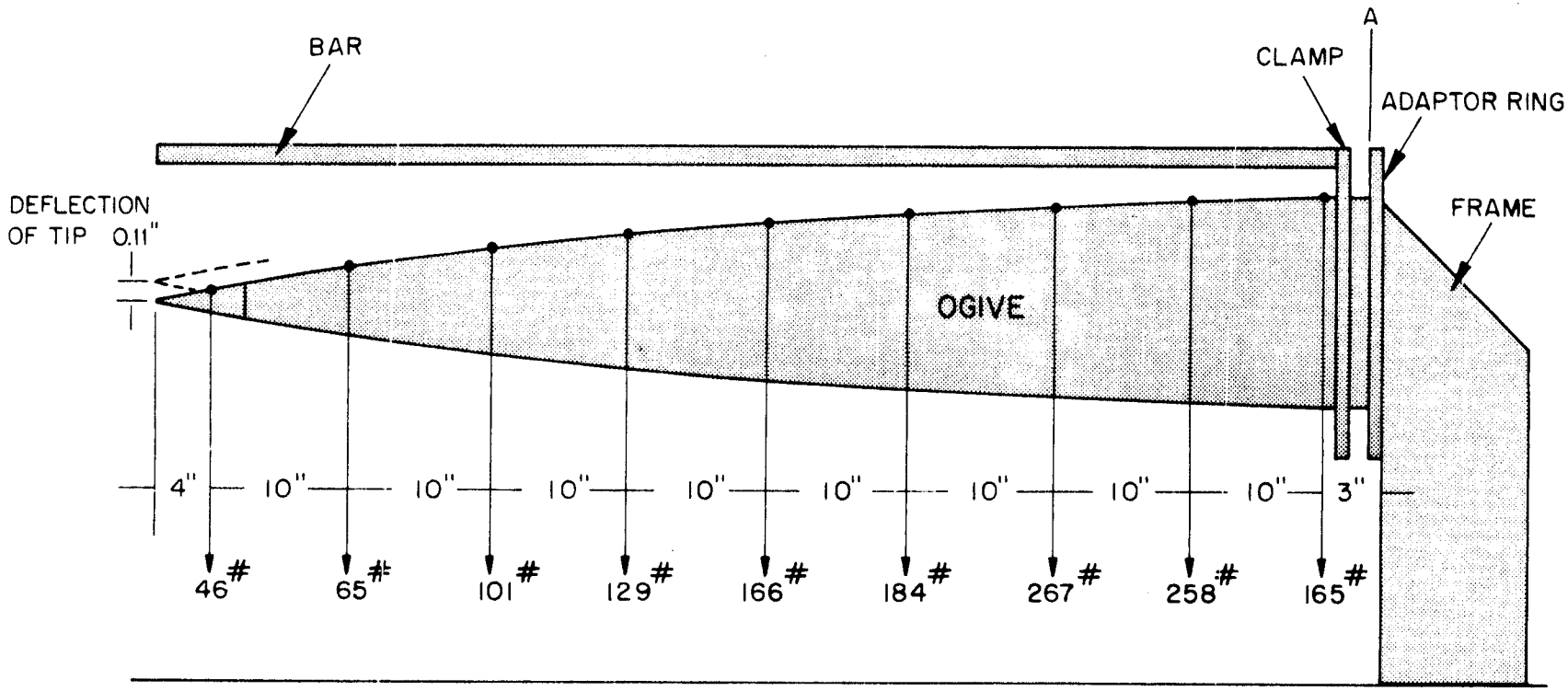

Figure 2

4.147CG OGIVE BENDING MOMENT TEST

During each vibration sequence the payload was operated in the same mode as during the rocket motor burning phase of the flight. The payload was in full operation on internal battery power and the electrical performance was recorded on strip charts. No adverse performance was noted.

After vibration in each axis the payload was inspected to the degree possible by viewing through doors and access parts. Upon completion of the test the payload was given a thorough mechanical inspection at AS&E.

Vacuum Tests

Both payloads, in completely assembled configuration, were subjected to a one hour vacuum test with vacuum in the 10^6 Torr range. The primary purpose of this test was to gain assurance that the completely assembled payload would be free of high voltage corona or high voltage arc discharge problems. During pump down the payload was operated while passing through the corona region. Upon achieving the desired vacuum level a complete electrical system test was conducted, including the operation of all pyrotechnic devices.

Payload/Telemetry Integration Tests

Payload/Telemetry Integration tests were conducted on both payloads at GSFC. The instrument payload was mated to the telemetry section, a complete simulated flight was conducted, and operational data was recorded by the GSFC telemetry ground station.

The integration tests for Aerobee 4.149 also included compatability and simulated flight tests with the ACS system.

Upon completion of the above tests the payloads were considered ready for flight. They were then subjected to a final calibration test at AS&E and shipped to White Sands Missile Range.

September, 1966
American Science and Engineering, Inc.
11 Carleton Street
Cambridge, Massachusetts, 02142